The expression study suggested that mutant HLCS with T462I or G581S showed less than 5% of the normal activity [Aoki et al., 1999]. We never found HLCS-deficient patients who harbor two null mutations. From these observations, we can speculate that homozygous null mutations are lethal in utero and combination of a null mutation and a point mutation that shows less than a few percent of the normal activity results in neonatal onset.

In eight clinically well-documented patients who have at least one allele of R508W, none displayed symptoms before the age of 2 months. Patients are biotin responsive and the prognosis was fine except in one case [Morrone et al., 2002]. This mutant enzyme's favorable response to biotin was also demonstrated by in vitro experiments [Dupuis et al., 1999]. Although the number of cases to study is still limited, patients with V550M are also expected to show good prognosis [Aoki et al., 1997; Morrone et al., 2002]. The IVS10+5G>A mutation shows a unique clinical character. Onset of the homozygotes of this mutation ranges from 2 months to 8 years (median 5 months) [Santer et al., 2003; Yang et al., 2001]. As previously noted, some patients homozygous for this mutation may be asymptomatic. In spite of a rather mild phenotype associated with IVS10+5G>A among HLCS-deficient patients at the onset, the clinical responses to biotin treatment are slow and partial in some cases [Holme et al., 1988; Santer et al., 2003].

In conclusion, there is a relationship between clinical biotin responsiveness and the residual activity of HLCS. We can predict the response to biotin therapy from genotypes in a patient who has a combination of well-characterized mutations stated above. However, we should be aware that some variation of outcome exists between patients with the same mutation.

DIAGNOSTIC RELEVANCE

Clinical pictures of HLCS deficiency and those of biotinidase deficiency are often indistinguishable. It is essential to perform enzymatic or DNA assays to identify the primary defect of patients who show MCD. Out of 16 HLCS-deficient Japanese patients from independent families, 15 have at least one allele of the four major mutations (del780C, L237P, R508W, and V550M). We routinely screen for these four mutations in our laboratory as the initial step for diagnosis of MCD in Japanese patients. If none of the four mutations are identified, we perform an enzyme assay [Suzuki et al., 1996]. In patients from ethnic groups other than the Faroese, mutations appear to be diverse. Thus, an enzyme assay is the first choice for the definitive diagnosis of HLCS deficiency in many ethnic groups. In the Faroese, DNA examination to detect IVS10+5G>T is useful.

FUTURE PROSPECTS

Information on HLCS mutations is still limited and further investigation into the mutation spectrum of each ethnic group is required to facilitate the diagnostic DNA examination of patients with MCD.

As exemplified by the recent works, roles of HLCS other than the biotinylation of carboxylases may exist [Narang et al., 2004; Solorzano-Vargas et al., 2002]. Newly identified functions of HLCS may be responsible for various symptoms observed in patients with HLCS deficiency.

Recently, a patient with MCD and a deficiency of the biotin transporter in the peripheral blood cells was reported [Mardach et al., 2002]. No abnormalities were found in biotinidase or HLCS, indicating that MCD can be caused by defects in three different primary substances: HLCS, biotinidase, and biotin transporter. We encountered patients who showed biotin-responsive MCD symptoms with normal HLCS and biotinidase activity (unpublished results). The *SMVT* gene coding for biotin transport had been investigated as a candidate disease-causing gene. However, the reported patient and our patients had no mutation in the gene (unpublished results) [Mardach et al., 2002]. Identification of the third gene that causes MCD remains to be elucidated in the field of human biotin metabolism.

ACKNOWLEDGMENTS

We thank the physicians who referred patients with HLCS deficiency. We also thank Kumi Kato for the excellent technical assistance.

REFERENCES

Achuta Murthy PN, Mistry SP. 1972. Synthesis of biotin-dependent carboxylases from their apoprotein and biotin. J Sci Ind Res (India) 31:554–563.

Aoki Y, Suzuki Y, Sakamoto O, Li X, Takahashi K, Ohtake A, Sakuta R, Ohura T, Miyabayashi S, Narisawa K. 1995. Molecular analysis of holocarboxylase synthetase deficiency: a missense mutation and a single base deletion are predominant in Japanese patients. Biochim Biophys Acta 1272:168–174.

Aoki Y, Suzuki Y, Li X, Sakamoto O, Chikaoka H, Takita S, Narisawa K. 1997. Characterization of mutant holocarboxylase synthetase (HCS): a Km for biotin was not elevated in a patient with HCS deficiency. Pediatr Res 42:849–854.

Aoki Y, Li X, Sakamoto O, Hiratsuka M, Akaishi H, Xu L, Briones P, Suormala T, Baumgartner ER, Suzuki Y, Narisawa K. 1999. Identification and characterization of mutations in patients with holocarboxylase synthetase deficiency. Hum Genet 104:143–148.

Baumgartner ER, Suormala T. 1997. Multiple carboxylase deficiency: inherited and acquired disorders of biotin metabolism. Int J Vitam Nutr Res 67:377–384.

Briones P, Ribes A, Vilaseca MA, Rodriguez-Valcarcel G, Thuy LP, Sweetman L. 1989. A new case of holocarboxylase deficiency. J Inherit Metab Dis 12:329–330.

Burri B, Sweetman L, Nyhan WL. 1985. Heterogeneity of holocarboxylase synthetase in patients with biotin-responsive multiple carboxylase deficiency. Am J Hum Genet 37:326–337.

Chikaoka H, Nagano M, Takita S, Shinka T, Kuhara T, Inoue Y, Matsumoto I. 1992. Multiple carboxylase deficiency: a case report. In: Matsumoto I, editor. Advances in chemical diagnosis and treatment of metabolic diseases. New York: John Willy & Sons. p 31–36.

Dupuis L, Leon-Del-Rio A, Leclerc D, Campeau E, Sweetman L, Saudubray JM, Herman G, Gibson KM, Gravel RA. 1996. Clustering of mutations in the biotin-binding region of holocarboxylase synthetase in biotin-responsive multiple carboxylase deficiency. Hum Mol Genet 5:1011–1016.

Dupuis L, Campeau E, Leclerc D, Gravel RA. 1999. Mechanism of biotin responsiveness in biotin-responsive multiple carboxylase deficiency. Mol Genet Metab 66:80–90.

Ewald H, Wang AG, Vang M, Mors O, Nyegaard M, Kruse TA. 1999. A haplotype-based study of lithium responding patients with bipolar affective disorder on the Faroe Islands. Psychiatr Genet 9:23–34.

Fuchshuber A, Suormala T, Roth B, Duran M, Michalk D, Baumgartner ER. 1993. Holocarboxylase synthetase deficiency: early diagnosis and management of a new case. Eur J Pediatr 152:446–449.

Gibson KM, Bennett MJ, Nyhan WL, Mize CE. 1996. Late-onset holocarboxylase synthetase deficiency. J Inherit Metab Dis 19:739–742.

Hattori M, Fujiyama A, Taylor TD, Watanabe H, Yada T, Park HS, Toyoda A, Ishii K, Totoki Y, Choi DK, Soeda E, Ohki M, Takagi T, Sakaki Y, Taudien S, Blechschmidt K, Polley A, Menzel U, Delabar J, Kumpf K, Lehmann R, Patterson D, Reichwald K, Rump A, Schillhabel M, Schudy A. 2000. The DNA sequence of human chromosome 21. The chromosome 21 mapping and sequencing consortium. Nature 405:311–319.

Hiratsuka M, Sakamoto O, Li X, Suzuki Y, Aoki Y, Narisawa K. 1998. Identification of holocarboxylase synthetase (HCS) proteins in human placenta. Biochim Biophys Acta 1385: 165–171.

Holme E, Jacobson CE, Kristiansson B. 1988. Biotin-responsive multiple carboxylase deficiency in an 8-year-old boy with normal serum biotinidase and fibroblast holocarboxylase-synthetase activities. J Inherit Metab Dis 11:270–276.

Hwu W, Suzuki Y, Yang X, Li X, Chou S, Narisawa K, Tsai W. 2000. Late-onset holocarboxylase synthetase deficiency with homologous R508W mutation. J Formos Med Assoc 99:174–177.

Leon-Del-Rio A, Leclerc D, Akerman B, Wakamatsu N, Gravel RA. 1995. Isolation of a cDNA encoding human holocarboxylase synthetase by functional complementation of a biotin auxotroph of Escherichia coli. Proc Natl Acad Sci USA 92: 4626–4630.

Mardach R, Zempleni J, Wolf B, Cannon MJ, Jennings ML, Cress S, Boylan J, Roth S, Cederbaum S, Mock DM. 2002. Biotin dependency due to a defect in biotin transport. J Clin Invest 109:1617–1623.

Morrone A, Malvagia S, Donati MA, Funghini S, Ciani F, Pela I, Boneh A, Peters H, Pasquini E, Zammarchi E. 2002. Clinical findings and biochemical and molecular analysis of four patients with holocarboxylase synthetase deficiency. Am J Med Genet 111:10–18.

Narang MA, Dumas R, Ayer LM, Gravel RA. 2004. Reduced histone biotinylation in multiple carboxylase deficiency patients: a nuclear role for holocarboxylase synthetase. Hum Mol Genet 13:15–23.

Narisawa K, Arai N, Igarashi Y, Satoh T, Tada K. 1982. Clinical and biochemical findings on a child with multiple biotin-responsive carboxylase deficiencies. J Inher Metab Dis 5:67–68.

Ohira M, Seki N, Nagase T, Suzuki E, Nomura N, Ohara O, Hattori M, Sakaki Y, Eki T, Murakami Y, and others. 1997. Gene identification in 1.6-Mb region of the Down syndrome region on chromosome 21. Genome Res 7:47–58.

Pacheco-Alvarez D, Solorzano-Vargas RS, Del Rio AL. 2002. Biotin in metabolism and its relationship to human disease. Arch Med Res 33:439–447.

Peters DM, Griffin JB, Stanley JS, Beck MM, Zempleni J. 2002. Exposure to UV light causes increased biotinylation of histones in Jurkat cells. Am J Physiol Cell Physiol 283:C878–C884.

Sakamoto O, Suzuki Y, Aoki Y, Li X, Hiratsuka M, Yanagihara K, Inui K, Okabe T, Yamaguchi S, Kudoh J, Shimizu N, Narisawa K. 1998. Molecular analysis of new Japanese patients with holocarboxylase synthetase deficiency. J Inherit Metab Dis 21:873–874.

Sakamoto O, Suzuki Y, Li X, Aoki Y, Hiratsuka M, Suormala T, Baumgartner ER, Gibson KM, Narisawa K. 1999. Relationship between kinetic properties of mutant enzyme and biochemical and clinical responsiveness to biotin in holocarboxylase synthetase deficiency. Pediatr Res 46:671–676.

Sakamoto O, Suzuki Y, Li X, Aoki Y, Hiratsuka M, Holme E, Kudoh J, Shimizu N, Narisawa K. 2000. Diagnosis and molecular analysis of an atypical case of holocarboxylase synthetase deficiency. Eur J Pediatr 159:18–22.

Santer R, Muhle H, Suormala T, Baumgartner ER, Duran M, Yang X, Aoki Y, Suzuki Y, Stephani U. 2003. Partial response to biotin therapy in a patient with holocarboxylase synthetase deficiency: clinical, biochemical, and molecular genetic aspects. Mol Genet Metab 79:160–166.

Solorzano-Vargas RS, Pacheco-Alvarez D, Leon-Del-Rio A. 2002. Holocarboxylase synthetase is an obligate participant in biotin-mediated regulation of its own expression and of biotin-dependent carboxylases mRNA levels in human cells. Proc Natl Acad Sci USA 99:5325–5330.

Stanley JS, Griffin JB, Zempleni J. 2001. Biotinylation of histones in human cells. Effects of cell proliferation. Eur J Biochem 268:5424–5429.

Suormala T, Fowler B, Duran M, Burtscher A, Fuchshuber A, Tratzmuller R, Lenze MJ, Raab K, Baur B, Wick H, Baumgartner ER. 1997. Five patients with a biotin-responsive defect in holocarboxylase formation: evaluation of responsiveness to biotin therapy in vivo and comparative biochemical studies in vitro. Pediatr Res 41:666–673.

Suormala T, Fowler B, Jakobs C, Duran M, Lehnert W, Raab K, Wick H, Baumgartner ER. 1998. Late-onset holocarboxylase synthetase-deficiency: pre- and post-natal diagnosis and evaluation of effectiveness of antenatal biotin therapy. Eur J Pediatr 157:570–575.

Suzuki Y, Aoki Y, Ishida Y, Chiba Y, Iwamatsu A, Kishino T, Niikawa N, Matsubara Y, Narisawa K. 1994. Isolation and characterization of mutations in the human holocarboxylase synthetase cDNA. Nat Genet 8:122–128.

Suzuki Y, Aoki Y, Sakamoto O, Li X, Miyabayashi S, Kazuta Y, Kondo H, Narisawa K. 1996. Enzymatic diagnosis of holocarboxylase synthetase deficiency using apo-carboxyl carrier protein as a substrate. Clin Chim Acta 251:41–52.

Tang NL, Hui J, Yong CK, Wong LT, Applegarth DA, Vallance HD, Law LK, Fung SL, Mak TW, Sung YM, Cheung KL, Fok TF. 2003. A genomic approach to mutation analysis of holocarboxylase synthetase gene in three Chinese patients with late-onset holocarboxylase synthetase deficiency. Clin Biochem 36: 145–149.

Touma E, Suormala T, Baumgartner ER, Gerbaka B, Ogier de Baulny H, Loiselet J. 1999. Holocarboxylase synthetase deficiency: report of a case with onset in late infancy. J Inherit Metab Dis 22:115–122.

Wolf B, Hsia YE, Sweetman L, Nyhan WL. 1981. Multiple carboxylase deficiency: clinical and biochemical improvement following neonatal biotin treatment. Pediatrics 68:113–118.

Wolf B. 2001. Disorders of biotin metabolism. In: Scriver CR, Beaudet AL, Sly WS, Valle D, editors. The metabolic and molecular basis of inherited disease. New York: McGraw-Hill. p 3935–3962.

Yang X, Aoki Y, Li X, Sakamoto O, Hiratsuka M, Gibson KM, Kure S, Narisawa K, Matsubara Y, Suzuki Y. 2000. Haplotype analysis suggests that the two predominant mutations in Japanese patients with holocarboxylase synthetase deficiency are founder mutations. J Hum Genet 45:358–362.

Yang X, Aoki Y, Li X, Sakamoto O, Hiratsuka M, Kure S, Taheri S, Christensen E, Inui K, Kubota M, Ohira M, Ohki M, Kudoh J, Kawasaki K, Shibuya K, Shintani A, Asakawa S, Minoshima S, Shimizu N, Narisawa K, Matsubra Y, Suzuki Y. 2001. Structure of human holocarboxylase synthetase gene and mutation spectrum of holocarboxylase synthetase deficiency. Hum Genet 109:526–534.

nature genetics

Germline *KRAS* and *BRAF* mutations in cardio-facio-cutaneous syndrome

Tetsuya Niihori[1], Yoko Aoki[1], Yoko Narumi[1], Giovanni Neri[2], Hélène Cavé[3], Alain Verloes[3], Nobuhiko Okamoto[4], Raoul C M Hennekam[5], Gabriele Gillessen-Kaesbach[6], Dagmar Wieczorek[6], Maria Ines Kavamura[7], Kenji Kurosawa[8], Hirofumi Ohashi[9], Louise Wilson[10], Delphine Heron[11], Dominique Bonneau[12], Giuseppina Corona[13], Tadashi Kaname[14], Kenji Naritomi[14], Clarisse Baumann[3], Naomichi Matsumoto[15], Kumi Kato[1,16], Shigeo Kure[1] & Yoichi Matsubara[1,16]

Cardio-facio-cutaneous (CFC) syndrome is characterized by a distinctive facial appearance, heart defects and mental retardation. It phenotypically overlaps with Noonan and Costello syndrome, which are caused by mutations in *PTPN11* and *HRAS*, respectively. In 43 individuals with CFC, we identified two heterozygous *KRAS* mutations in three individuals and eight *BRAF* mutations in 16 individuals, suggesting that dysregulation of the RAS-RAF-ERK pathway is a common molecular basis for the three related disorders.

Cardio-facio-cutaneous (CFC) syndrome (OMIM 115150) was first described in 1986 (ref. 1). Affected individuals present with heart defects, including pulmonic stenosis, atrial septal defects and hypertrophic cardiomyopathy, and ectodermal abnormalities such as sparse, friable hair, hyperkeratotic skin lesions and a generalized ichthyosis-like condition. Typical facial characteristics include high forehead with bitemporal constriction, hypoplastic supraorbital ridges, downslanting palpebral fissures, a depressed nasal bridge and posteriorly angulated ears with prominent helices. The molecular basis of CFC syndrome has remained unknown. There are phenotypic similarities between this syndrome, Noonan syndrome (OMIM 163950) and Costello syndrome (OMIM 218040)[2,3]. Gain-of-function mutations in protein tyrosine phosphatase SHP-2 (*PTPN11*) have been identified in approximately 40% of individuals with clinically diagnosed Noonan syndrome[4]. No *PTPN11* mutations have been found in individuals with CFC syndrome[5–7]. Recently, we identified *HRAS* mutations in 12 of 13 individuals with Costello syndrome[8]. These findings suggest that the activation of the RAS-MAPK pathway is the common underlying mechanism of Noonan syndrome and Costello syndrome and, hence, possibly of CFC syndrome.

To elucidate the molecular basis of CFC syndrome, we first sequenced the entire coding regions of three RAS genes, *HRAS* (NC_000011), *KRAS* (NC_000012) and *NRAS* (NC_000001), in genomic DNA from 43 individuals with CFC syndrome (**Supplementary Methods** online). We identified two *KRAS* mutations: G60R (178G→C) in CFC73 and D153V (458A→T) in CFC8 and CFC91 (**Fig. 1a** and **Table 1**). Neither mutation has been previously identified in individuals with cancer (Sanger Institute Catalogue of Somatic Mutations in Cancer (COSMIC); http://www.sanger.ac.uk/cosmic). Gly60 and Asp154 are evolutionally conserved or chemically similar (**Supplementary Fig. 1** online). Neither of the two mutations was observed in 100 control chromosomes (data not shown). Their parents did not carry the mutations (**Supplementary Fig. 1**). The D153V mutation was identified in DNA extracted from both blood and buccal cells of individual CFC91. These results suggest that these germline mutations occurred *de novo*. No mutations in *KRAS*, *NRAS* or *HRAS* were found in the other 40 individuals with CFC syndrome.

Next, we examined the downstream molecules of RAS in the signaling pathway. The *RAF* proto-oncogene family consists of three isoforms, *CRAF*, *BRAF* and *ARAF*, and encodes for cytoplasmic serine/threonine kinases that are activated by binding RAS. Among these RAF molecules, BRAF is expressed at high levels in the brain and mutations in *BRAF* have been identified in 7% of all cancers[9]. We sequenced the entire 18 coding exons of *BRAF* (NC_000007) in 40 individuals with CFC syndrome and identified eight mutations in sixteen individuals (**Table 1**). Six mutations were located in the kinase domain (**Fig. 1b**). A G469E (1406G→A) mutation, which resides in the glycine-rich loop where somatic mutations are clustered in cancer, was identified in four individuals (CFC76, CFC81, CFC94 and CFC114). N581D (1741A→G), located in the catalytic loop, was identified in CFC95 and CFC110. Four mutations in the kinase domain between the glycine-rich loop and the catalytic loop were identified in five affected individuals: L485F (1455G→C) in CFC83, K499E (1495A→G) in CFC79, E501K (1501G→A) in CFC77 and E501G (1502A→G) in CFC90 and CFC105. A246P (736G→C) and

[1]Department of Medical Genetics, Tohoku University School of Medicine, Sendai, Japan. [2]Università Cattolica, Istituto di Genetica Medica, Rome, Italy. [3]Department of Genetics, Hôpital Robert Debré (APHP), Paris, France. [4]Department of Planning and Research, Osaka Medical Center and Research Institute for Maternal and Child Health, Izumi, Osaka, Japan. [5]Clinical and Molecular Genetics Unit, Institute of Child Health, London, UK and Department of Pediatrics, Academic Medical Center, Amsterdam, Netherlands. [6]Institut für Humangenetik, Universität Essen, Essen, Germany. [7]Medical Genetics Center, Federal University of Sao Paulo (UNIFESP), Sao Paulo, Brazil. [8]Division of Medical Genetics, Kanagawa Children's Medical Center, Yokohama, Japan. [9]Division of Medical Genetics, Saitama Children's Medical Center, Saitama, Japan. [10]Great Ormond Street Hospital, London, UK. [11]Genetic Department, Pitie-Salpetriere University Hospital, Paris, France. [12]Genetic Department, University Hospital, Angers, France. [13]Unità Operativa Complessa Patologia Neonatale e Terapia Intensiva, Dipartimento di Scienze Pediatriche Mediche e Chirurgiche, Azienda Ospedaliera Universitaria G. Martino, Messina, Italy. [14]Department of Medical Genetics, University of the Ryukyus School of Medicine, Okinawa, Japan. [15]Department of Human Genetics,Yokohama City University Graduate School of Medicine, Yokahama, Japan. [16]Comprehensive Research and Education Center for Planning of Drug Development and Clinical Evaluation, 21st Century COE Program, Tohoku University, Sendai, Japan. Correspondence should be addressed to Y.A. (aokiy@mail.tains.tohoku.ac.jp).

Received 20 November 2005; accepted 17 January 2006; published online 12 February 2006; doi:10.1038/ng1749

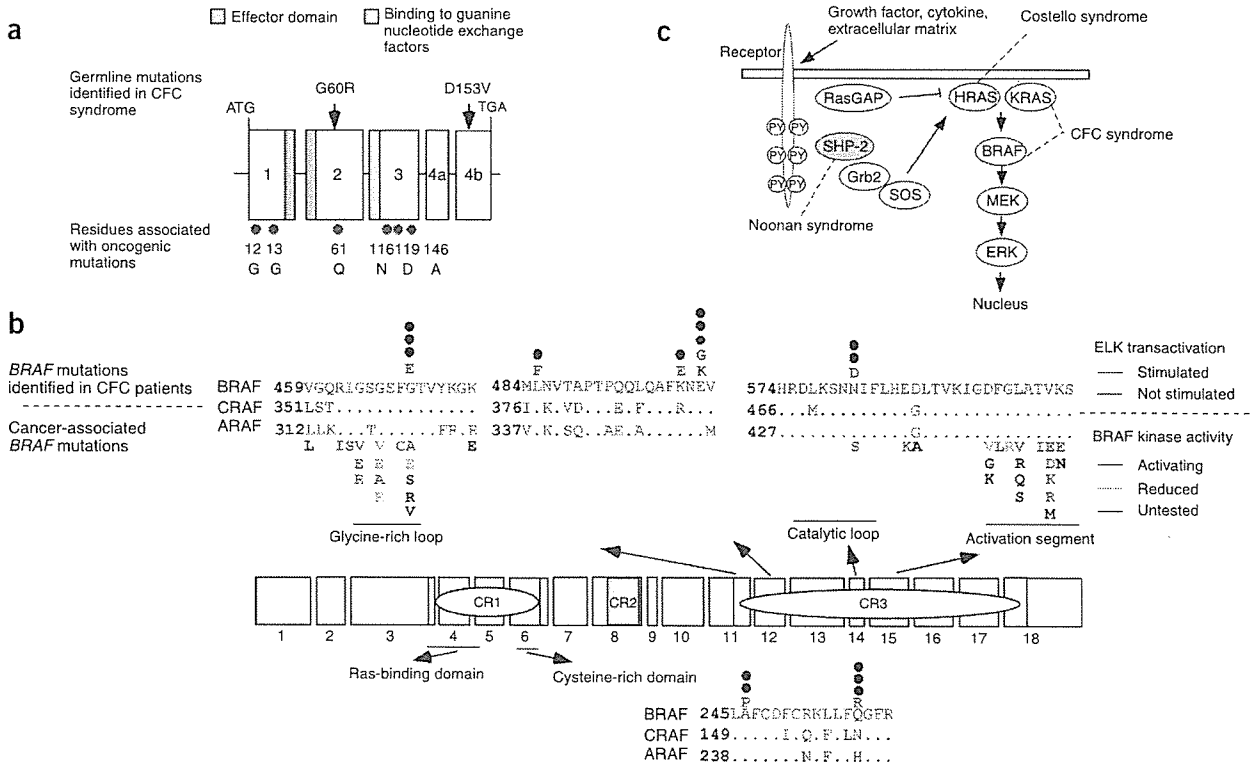

Figure 1 Mutations in *KRAS* and *BRAF* were identified in individuals with CFC syndrome. (**a**) Domain organization and genomic structure of the *KRAS* gene. Coding exons are numbered. In 98% of the transcripts, exon 4a is spliced out and only exon 4b is available for translation into protein. (**b**) *BRAF* consists of 18 exons. The three regions conserved in all RAF proteins (conserved region (CR) 1, CR2, and CR3) are shown in blue, green and yellow, respectively. The kinase domain is located in the CR3 domain. Six substitutions identified in CR3 are shown above. Filled circles indicate number of individuals having the substitution. Cancer-associated *BRAF* mutations are shown below the alignment of three RAF proteins[9,12]. Mutations detected in cancer are clustered in the glycine-rich loop and the activation segment of CR3 domain. The V600E mutation accounts for over 90% of the mutations in melanoma and thyroid cancer. Two mutations in the cysteine-rich domain were identified in five CFC individuals. Amino acids in CRAF and ARAF that are conserved in BRAF are shown by dots[13]. (**c**) RAS-ERK signaling pathway and associated disorders. RAS binds and stimulates RAF activation, which then activates MEK, which in turn activates ERK. ERK regulates gene expression and cytoskeletal rearrangements to coordinate the response to extracellular signals and regulate proliferation, differentiation, senescence and apoptosis[8,9]. Substitutions in *PTPN11*, *HRAS*, *KRAS* or *BRAF*, which potentially dysregulate the RAS-ERK signaling pathway, account for similar developmental disorders.

Q257R (770A→G), located in the cysteine-rich domain, were identified in five patients (**Fig. 1b** and **Table 1**). The identified eight substitutions were not found in 100 control chromosomes (data not shown). Mutation analysis in parents of five individuals (CFC76, CFC77, CFC96, CFC103 and CFC114) showed that these mutations occurred *de novo* (**Supplementary Fig. 2** online). The identified *BRAF* mutations were located in exons 6, 11, 12 and 14, and these domains were highly conserved in *CRAF* and *BRAF*. Sequencing of four corresponding exons in *CRAF*, ubiquitously expressed RAF, did not show any mutations in 24 individuals (data not shown).

KRAS and BRAF molecules are the key regulators of the RAS-RAF-MEK-ERK pathway, which is important for proliferation, growth and death of cells[9]. To elucidate critical steps, we examined the effect of the identified mutations on the RAS-ERK pathway by studying the activation of the ELK transcription factor. We transfected expression constructs (*KRAS* cDNA, NM_004985; *BRAF* cDNA, NM_00433) with a pFR-luc *trans*-reporter vector, a pFA2-ELK1 vector and a phRLnull-luc vector in NIH3T3 cells and determined their relative luciferase activity (RLA). We observed a significant increase in RLA in cells transfected with *KRAS* D153V but not in cells transfected with *KRAS* G60R (**Supplementary Fig. 3** online). We observed a two- to fourfold increase in RLA in cells transfected with two *BRAF* mutations (A246P and Q257R) in the cysteine-rich domain as well as in cells transfected with two *BRAF* mutations (L485S and K499E) in the kinase domain. We did not observe any significant increase in RLA in the other four mutations. Protein blotting showed that the wild-type and mutant proteins of *KRAS* and *BRAF* were equally expressed (data not shown). These results suggest that one *KRAS* and four *BRAF* mutants identified in CFC syndrome stimulated a common signaling pathway.

We identified substitutions of two proto-oncogenes, *KRAS* and *BRAF*, in 44% of individuals with CFC syndrome, suggesting that *KRAS* and *BRAF* have similar roles in human development. Controversy has existed as to whether CFC and Noonan syndromes are distinct disorders or different phenotypes of the same condition[2,10]. The clinical data of the 19 mutation-positive CFC individuals showed a high frequency of growth failure (78.9%), mental retardation (100%), relative macrocephaly (78.9%), characteristic facial appearance, including bitemporal constriction (84.2%) and downslanting palpebral fissures (94.7%), curly sparse hair (100%), heart defects (84.2%) and skin abnormalities (68.4%) (**Supplementary Table 1** online). This is in contrast with Noonan syndrome, in which there are lower frequencies of mental retardation (24–35%), heart defects (50–67%) and skin

Table 1 Mutations in 19 individuals with CFC syndrome

Individual	Gene	Exon	Nucleotide substitution	Amino acid change
CFC73	KRAS	2	178G→C	G60R
CFC8	KRAS	4b	458A→T	D153V
CFC91	KRAS	4b	458A→T	D153V
CFC100	BRAF	6	736G→C	A246P
CFC103	BRAF	6	736G→C	A246P
CFC16	BRAF	6	770A→G	Q257R
CFC24	BRAF	6	770A→G	Q257R
CFC96	BRAF	6	770A→G	Q257R
CFC76	BRAF	11	1406G→A	G469E
CFC81	BRAF	11	1406G→A	G469E
CFC94	BRAF	11	1406G→A	G469E
CFC114	BRAF	11	1406G→A	G469E
CFC83	BRAF	12	1455G→C	L485F
CFC79	BRAF	12	1495A→G	K499E
CFC77	BRAF	12	1501G→A	E501K
CFC90	BRAF	12	1502A→G	E501G
CFC105	BRAF	12	1502A→G	E501G
CFC95	BRAF	14	1741A→G	N581D
CFC110	BRAF	14	1741A→G	N581D

abnormalities (2–27%)[2]. Mutation analysis of *PTPN11* was negative in 43 CFC individuals. We did not identify any mutations in any exons of *KRAS* or in exons 6, 11, 12 and 14 of *BRAF* in 26 individuals with *PTPN11*-negative Noonan syndrome (data not shown), suggesting that Noonan syndrome and CFC syndrome are distinct clinical entities.

Comparison of manifestations between *KRAS*-positive and *BRAF*-positive individuals showed similar frequencies of growth and mental retardation, craniofacial appearance, abnormal hair and heart defects (**Supplementary Tables 2** and **3** online). However, we did observe a difference between the two groups in manifestations of skin abnormality, including ichthyosis, hyperkeratosis and hemangioma, which were observed in 13 *BRAF*-positive individuals. In contrast, no *KRAS*-positive individuals had these skin problems ($P < 0.05$). Somatic mutations in *BRAF* were identified in 60% of malignant melanoma or nevi[9], suggesting that BRAF has an important role in the skin. Comparison of manifestations between individuals with mutations that induced ELK transactivation and those with mutations that did not induce ELK transactivation showed no significant differences. Further analysis in a larger cohort would clarify the genotype-phenotype relationship in affected individuals.

The crystal structure of the BRAF kinase domain showed that the six *BRAF* mutations identified in this study are located in the interface of the ATP binding cleft, suggesting that these mutations may alter the catalytic activity of kinase domain (**Supplementary Fig. 4** online). Luciferase assays showed that two mutations (L485F and K499E) stimulated ELK-dependent transcription, suggesting that these mutants activated the ERK pathway. Missense mutations of *BRAF* were identified in approximately 7% of cancers, including human malignant melanoma and colorectal cancer[9]. The most frequent (>90%) V600E mutant showed elevated kinase activity, resulting in the activation of ERK and increased transformation activity[11]. Other less frequent mutations identified in cancer had either elevated or reduced kinase activity[9]. The four mutations identified in the kinase domain in our study did not enhance ELK-dependent transcription. This is in agreement with recent studies reporting that the activation of ERK or ELK transcription was not observed in cancer-associated mutations, including G469E (ref. 12). In cancer, *BRAF* mutations other than V600E are sometimes coincident with *RAS* mutations[9]. Other genetic background may contribute to the pathogenesis of CFC syndrome, although we did not detect any mutations in *KRAS*, *HRAS* or *NRAS* in *BRAF*-positive individuals. Further functional analysis of *BRAF* mutations will help elucidate the effects of these mutations on cell signaling.

The A246P and Q257R mutations are the first to be identified in the cysteine-rich domain in *BRAF*. This cysteine-rich domain is adjacent to the RAS-binding domain in conserved region 1 (ref. 13). A past study has suggested that the cysteine-rich domain of CRAF not only binds activated small GTPase RAS, but also inhibits basal catalytic RAF activity by direct or indirect interaction with the catalytic domain[14]. Our luciferase assay showed that these two mutations significantly activated ELK-dependent transcription, suggesting that they contribute to the activation of *BRAF*, leading to stimulation of the RAS-ERK pathway.

Previous clinical reports have shown that the association with cancers is rare in CFC syndrome[15]. This is in contrast with individuals with Costello syndrome, who have a higher risk of cancer, including rhabdomyosarcoma, ganglioneuroblastoma and bladder carcinoma[8]. It is of note that individual CFC94 with a *BRAF* G469E mutation had acute lymphoblastoid leukemia[15]. Careful observation of affected individuals would clarify the possible predisposition to hematopoietic malignancy in CFC syndrome as described in Noonan syndrome[4].

To the best of our knowledge, this is the first report of germline mutations in *KRAS* and *BRAF*. Our results suggest that mutations in human oncogenes (*HRAS*, *KRAS*, *BRAF* and *PTPN11*) that potentially dysregulate the RAS-MAPK pathway represent a common fundamental mechanism of related developmental disorders, namely, Noonan syndrome, Costello syndrome and CFC syndrome (**Fig. 1c**).

GenBank accession numbers. *KRAS* coding region, NC_000012; *HRAS* coding region, NC_000011; *NRAS* coding region, NC_000001; *BRAF*, NC_000007; *KRAS* cDNA, NM_004985; *BRAF* cDNA, NM_004333.

Note: Supplementary information is available on the Nature Genetics website.

ACKNOWLEDGMENTS

We wish to thank the individuals and their families who participated in this study and the doctors who referred the cases. The support of CFC International in facilitating the collection of patient samples is gratefully acknowledged. We are grateful to J. Miyazaki, Osaka University, for supplying the pCAGGS expression vector. This work was supported by Grants-in-Aid from the Ministry of Education, Culture, Sports, Science and Technology of Japan and Grants-in-Aid from the Ministry of Health, Labor, and Welfare of Japan.

COMPETING INTERESTS STATEMENT

The authors declare that they have no competing financial interests.

Published online at http://www.nature.com/naturegenetics
Reprints and permissions information is available online at http://npg.nature.com/reprintsandpermissions/

1. Reynolds, J.F. *et al. Am. J. Med. Genet.* **25**, 413–427 (1986).
2. Wieczorek, D., Majewski, F. & Gillessen-Kaesbach, G. *G. Clin. Genet.* **52**, 37–46 (1997).
3. van Eeghen, A.M., van Gelderen, I. & Hennekam, R.C. *Am. J. Med. Genet.* **82**, 187–193 (1999).
4. Tartaglia, M. & Gelb, B.D. *Eur. J. Med. Genet.* **48**, 81–96 (2005).
5. Ion, A. *et al. Hum. Genet.* **111**, 421–427 (2002).
6. Kavamura, M.I. *et al. Eur. J. Hum. Genet.* **11**, 64–68 (2003).
7. Musante, L. *et al. Eur. J. Hum. Genet.* **11**, 201–206 (2003).
8. Aoki, Y. *et al. Nat. Genet.* **37**, 1038–1040 (2005).
9. Garnett, M.J. & Marais, R. *Cancer Cell* **6**, 313–319 (2004).
10. Neri, G., Zollino, M. & Reynolds, J.F. *Am. J. Med. Genet.* **39**, 367–370 (1991).
11. Davies, H. *et al. Nature* **417**, 949–954 (2002).
12. Ikenoue, T. *et al. Cancer Res.* **64**, 3428–3435 (2004).
13. Mercer, K.E. & Pritchard, C.A. *Biochim. Biophys. Acta* **1653**, 25–40 (2003).
14. Winkler, D.G. *et al. J. Biol. Chem.* **273**, 21578–21584 (1998).
15. van Den Berg, H. & Hennekam, R.C. *J. Med. Genet.* **36**, 799–800 (1999).

Original Article

Association between Carotid Hemodynamics and Asymptomatic White and Gray Matter Lesions in Patients with Essential Hypertension

Mie KURATA, Takafumi OKURA, Sanae WATANABE, and Jitsuo HIGAKI

The aim of this study was to clarify the magnitude of common carotid artery (CCA) structural and hemodynamic parameters on brain white and gray matter lesions in patients with essential hypertension (EHT). The study subjects were 49 EHT patients without a history of previous myocardial infarction, atrial fibrillation, diabetes mellitus, impaired glucose tolerance, chronic renal failure, symptomatic cerebrovascular events, or asymptomatic carotid artery stenosis. All patients underwent brain MRI and ultrasound imaging of the CCA. MRI findings were evaluated by periventricular hyperintensity (PVH), deep and subcortical white matter hyperintensity (DSWMH), and état criblé according to the Japanese Brain dock Guidelines of 2003. Intima media thickness (IMT), and mean diastolic (V_d) and systolic (V_s) velocities were evaluated by carotid ultrasound. The V_d/V_s ratio was further calculated as a relative diastolic flow velocity. The mean IMT and max IMT were positively associated with PVH, DSWMH, and état criblé (mean IMT: ρ=0.473, 0.465, 0.494, p=0.0007, 0.0014, 0.0008, respectively; max IMT: ρ=0.558, 0.443, 0.514, p=0.0001, 0.0024, 0.0004, respectively). V_d/V_s was negatively associated with état criblé (ρ=−0.418, p=0.0038). Carotid structure and hemodynamics are potentially related to asymptomatic lesions in the cerebrum, and might be predictors of future cerebral vascular events in patients with EHT. (*Hypertens Res* 2005; 28: 797–803)

Key Words: **essential hypertension, asymptomatic lesions, white matter lesions, deep gray matter lesions, Doppler ultrasound**

Introduction

Recently, MRI studies have rendered it possible to assess asymptomatic cerebral white matter lesions and basal ganglial change. White matter lesions are generally considered to be associated with a high risk of stroke (*1–3*). Numerous studies have demonstrated that age and hypertension are highly and independently correlated with white matter lesions, periventricular hyperintensity (PVH) and subcortical white matter hyperintensity (DSWMH) (*4–7*). The incidence of a type of ganglial gray matter lesion, état criblé, has also been reported to be increased with aging and has been associated with hypertension (*8*).

Prospective population-based studies in Europe and the United States have reported that carotid intima-media thickness (IMT) and plaques diagnosed by ultrasound (US) imaging are positively associated with a subsequent occurrence of stroke (*9–12*). The aim of the current study was to clarify the relationship between the hemodynamics and the structure of the common carotid artery (CCA) and white and gray matter lesions in the brain of patients with essential hypertension (EHT).

From the Second Department of Internal Medicine, Ehime University School of Medicine, Toon, Japan.
Address for Reprints: Takafumi Okura, M.D., Ph.D., Second Department of Internal Medicine, Ehime University School of Medicine, Shitsukawa, Toon 791–0295, Japan. E-mail: okura@m.ehime-u.ac.jp
Received May 6, 2005; Accepted in revised form August 7, 2005.

Table 1. Clinical Characteristics of Participants

N (male/female)	49 (27/22)
Age (years)	58.7±15.6
BMI (kg/m^2)	25.2±4.6
SBP (mmHg)	153±23
DBP (mmHg)	87±15
Pulse pressure (mmHg)	65±19
Pulse (beats/min)	74±12
Mean 24-h SBP (mmHg)	140±16
Mean 24-h DBP (mmHg)	85±16
TC (mg/dl)	203±36
HDL-C (mg/dl)	52.9±15.8
FBG (mg/dl)	93.1±13.5
Smoking (yes/no)	24/25

BMI, body mass index; SBP, systolic blood pressure; DBP, diastolic blood pressure; TC, total cholesterol; HDL-C, high-density lipoprotein cholesterol; FBG, fasting blood glucose. Values are mean±SD.

Table 2. Vascular Wall and Hemodynamic Characteristics of Common Carotid Artery in Participants

Mean IMT (mm)	0.78±0.17
Max IMT (mm)	0.90±0.23
Plaque number	0.41±0.78
D_s (mm)	7.06±0.93
D_d (mm)	6.57±0.92
Arterial strain (%)	6.97±3.16
β	10.2±7.6
V_s (cm/s)	41.6±12.8
V_d (cm/s)	19.7±7.1
V_d/V_s	0.47±0.07
PI	1.92±0.50
RI	0.76±0.07

IMT, intima-media thickness; D_s, end-systolic diameter; D_d, end-diastolic diameter; β, carotid arterial stiffness index; V_s, mean systolic velocity; V_d, mean diastolic verocity; V_d/V_s, relative diastolic flow velocity; PI, pulsatility index; RI, resistive index. Values are mean±SD.

Methods

Study Population

Forty-nine hospitalized patients with EHT participated in this study. Hypertension was defined as systolic blood pressure (SBP) ≥140 mmHg or diastolic blood pressure (DBP) ≥90 mmHg, averaged by a three-fold determination and measured using a brachial sphygmomanometer while the patient was sitting down. The participants were recruited from consecutive cases that were admitted to Ehime University Hospital for the evaluation of hypertension. Patients with congestive heart failure, previous myocardial infarction, atrial fibrillation, diabetes mellitus (fasting blood glucose [FBG] level >126 mg/dl), impaired glucose tolerance (FBG level <126 mg/dl, and oral glucose tolerance test [OGTT] 2-h data >200 mg/dl), chronic renal failure (serum creatinine ≥3.0 mg/dl), or history of stroke were excluded from the study. All subjects received a diet containing 7 g of NaCl per day, and all medications were discontinued on admission. All procedures were performed after a stabilization period of at least 2 weeks. Informed consent was obtained from each subject for blood sampling and ultrasound evaluation. All patients agreed to undergo an MRI study of the brain.

Blood Sampling

Measurement of total cholesterol (TC), high-density lipoprotein cholesterol (HDL-C), and FBG were carried out using an automatic analyzer (model TBA-60S; Toshiba Inc., Tokyo, Japan).

Intermittent 24-h Ambulatory Blood Pressure Monitoring (ABPM)

Twenty-four-hour SBP and DBP were measured by a cuff-oscillometric method using an FB-250 oscillometer (Fukuda Denshi Co., Tokyo, Japan). Blood pressure was measured every 30 min from 6:00 AM to 10:00 PM and every 60 min from 10:00 PM to 6:00 AM of the following day.

Ultrasound Evaluation

Ultrasound evaluation of the CCA was performed with an SSD-2000 (Aloka Co., Tokyo, Japan) using a 7.5-MHz probe equipped with a Doppler system, as described previously (*13*). After the subjects had rested in the supine position for at least 10 min with the neck in slightly hyperextended position, we performed optimal bilateral visualization of the carotid artery. Based on multiple visualizations, plaque formation was identified as the presence of a wall thickening that was at least 50% greater than the thickness of the surrounding wall (*13*, *14*). The IMT of the far wall was measured in the CCA at both 1 and 2 cm proximal to the bulb from the anterior, lateral, and posterior approaches, and then was averaged to obtain the mean IMT values (*13*, *14*). No measurements were carried out at the level of discrete plaques.

Two-dimensional guided M-mode tracing of the right CCA at a point 2 cm proximal to the bulb was recorded simultaneously by both electrocardiogram and phonocardiogram. M-mode images were obtained in real time using a frame grabber. The axial resolution of the M-mode system was 0.1 mm. The internal diameter of the CCA at end-diastole (D_d) and peak-systole (D_s) was determined by continuous tracing of the intimal-luminal interface of the near and far walls of the

Table 3. Rank Correlation Coefficients (Risk Factors)

	PVH	DSWMH	État criblé
Age	0.643‡	0.558†	0.591‡
BMI	−0.188	−0.182	−0.053
SBP	0.194	0.071	0.112
DBP	−0.238	−0.273	−0.302
PP	0.446†	0.321	0.348
Mean 24-h SBP	0.115	0.074	0.092
Mean 24-h DBP	−0.190	−0.144	−0.292
TC	−0.016	−0.073	−0.127
HDL-C	0.157	0.158	0.169
FBG	0.080	0.138	0.141
Smoking	0.328	−0.142	−0.171

PVH, periventricular hyperintensity; DSWMH, deep subcortical white matter hyperintensity; BMI, body mass index; SBP, systolic blood pressure; DBP, diastolic blood pressure; PP, pulse pressure; TC, total cholesterol; HDL-C, high-density lipoprotein cholesterol; FBG, fasting blood glucose. †$p<0.01$, ‡$p<0.001$.

Table 4. Rank Correlation Coefficients (Ultrasound Parameters)

	PVH	DSWMH	État criblé
Mean IMT	0.473†	0.465†	0.494†
Max IMT	0.558‡	0.443*	0.514†
Plaque number	0.356	0.300	0.247
D_s	0.210	0.091	0.324
D_d	0.203	0.102	0.344
Arterial strain	−0.104	−0.135	−0.328
β	0.291	0.290	0.345
V_s	−0.071	−0.049	−0.192
V_d	−0.193	−0.131	−0.353
V_d/V_s	−0.309	−0.220	−0.418†
PI	−0.166	−0.170	−0.010
RI	0.113	0.055	0.254

IMT, intima-media thickness; D_s, end-systolic diameter; D_d, end-diastolic diameter; β, carotid arterial stiffness index; V_s, mean systolic velocity; V_d, mean diastolic verocity; V_d/V_s, relative diastolic flow velocity; PI, pulsatility index; RI, resistive index. *$p<0.05$, †$p<0.01$, ‡$p<0.001$.

CCA in three cycles, and the results were averaged (*13*). The cross-sectional distensibility coefficient (CSDC) and the carotid arterial stiffness index (β) were calculated using the following formulae (*12*, *15*).

$$\text{CSDC} = (D_s^2 - D_d^2)/[D_d^2 \times (\text{SBP} - \text{DBP})]$$

$$\beta = \ln(\text{SBP/DBP}) \times [D_d/(D_s - D_d)]$$

Doppler evaluation was performed by scanning the right CCA in the anterior projection. Under guidance using color flow mapping, the sample volume was located at the center of the vessel. Flow velocity-time integrals of the systolic and diastolic phases were computed automatically by electronic integration of the instantaneous flow velocity curves, and further systolic (V_s) to diastolic flow velocity (V_d) values were calculated to assess the hemodynamics in the CCA (*12*).

MRI

MRI was performed in all patients with a superconducting magnet with a main field strength of 1.5 T in order to evaluate the asymptomatic cerebrovascular damage. The MRI findings were classified according to the following parameters: PVH, DSWMH, and état criblé, according to the Japanese Brain-dock Guidelines 2003 (*15*).

PVH and DSWMH were defined as exhibiting high intensity lesions by T_2-weighted and proton density images or by fluid-attenuated inversion recovery (FLAIR) (*16*, *17*), and low intensity determined by T_1-weighted images. État criblé was assessed at the basal ganglial level, as high-intensity signals evaluated by T_2-weighted images (*18*).

PVH exhibits white matter hyperintensities (WMHIs) in contact with the ventricular wall. PVH were further classified as follows. 0: absent or only a "rim"; 1: limited lesion-like "caps"; 2: irregular "halo"; 3: irregular margins and extension into the deep white matter; 4: extension into the deep white matter and the subcortical portion.

DSWMH indicates WMHIs that are separated from the ventricular wall by a strip of normal-appearing white matter; these WMHIs were situated in the deep white matter and were sparsely present in the subcortical U-fiber region. DSWMH were further classified as follows. 0: absent; 1: ≤3 mm, small foci and regular margins; 2: ≥3 mm, large foci; 3: diffusely confluent; 4: extensive changes in the white matter.

État criblé was found to be <3 mm, with small focal points and regular margins in the basal ganglia. État criblé was further classified as follows. 0: absent; 1: 1–5 dots; 2: 6–10 dots; 3: ≥11 dots.

A lacuna was defined as an area of low signal intensity ≥3 mm and ≤15 mm by T_1-weighted proton density images, or an area of high intensity by T_2-weighted proton density images or FLAIR.

One of the present authors (M.K.) interpreted all of the MRI in a manner blinded with respect to the clinical status of the subjects.

Statistical Analysis

All values are expressed as the means±SD. Spearman's rank correlation coefficient was used to test the association. The Kruskal-Wallis test was used to compare differences among groups. Stepwise regression analysis was used to evaluate the independent parameters for PVH, DSWMH, and état criblé. Values of $p<0.05$ were considered to be statistically significant.

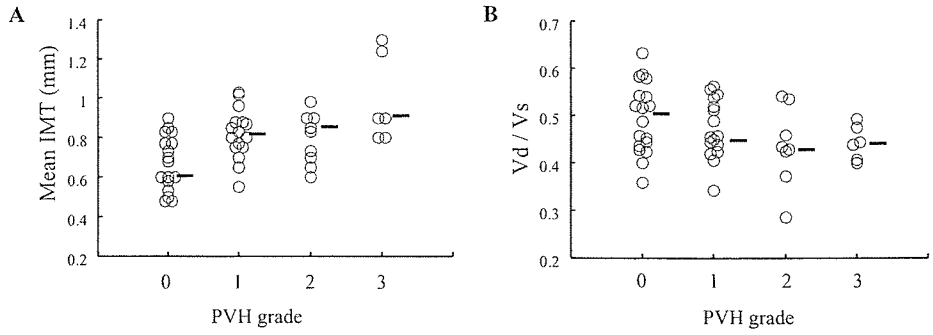

Fig. 1. *The relationship between PVH grades and IMT (A) and relative diastolic velocity (V_d/V_s) (B). PVH grades were positively correlated with mean IMT. IMT, intima-media thickness; PVH, periventricular hyperintensity;* ▬, *mean values of mean IMT and* V_d/V_s.

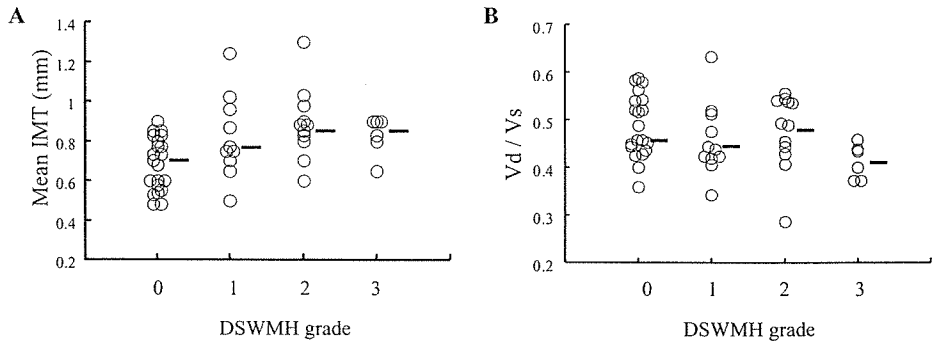

Fig. 2. *The relationship between DSWMH grades and IMT (A) and relative diastolic velocity (B). DSWMH was positively correlated with mean IMT. DSWMH, deep and subcortical white matter hyperintensity,* ▬, *mean values of mean IMT and* V_d/V_s.

Results

Patient Characteristics

Table 1 summarizes the characteristics of all hypertensive subjects included in the present study, and the hemodynamics and structure of CCA are summarized in Table 2.

Rank Correlation Coefficients between Risk Factors and MRI Findings

The numbers of patients with PVH grades 0, 1, 2, 3, and 4 were 18, 16, 9, 6, and 0, respectively. DSWMH grades 0, 1, 2, 3, 4 were observed in 21, 10, 12, 6, and 0 patients, respectively. The état criblé grades 0, 1, 2, and 3 were observed in 16, 20, 8, and 5 patients, respectively. The relationships between each of age, SBP, DBP, pulse pressure (PP) and TC and each of PVH, DSWMH, and état criblé are summarized in Table 3. Age was positively associated with PVH, DSWMH, and état criblé (ρ=0.643, 0.558, and 0.591, at $p<0.0001$, <0.0001, and <0.0001, respectively). PP was positively associated with PVH (ρ=0.446, p=0.002).

Rank Correlation Coefficients between US Parameters and MRI Grades

The relationships between carotid US parameters and PVH, DSWMH, and état criblé are summarized in Table 4. The mean IMT and max IMT were positively associated with PVH, DSWMH, and état criblé (mean IMT: ρ=0.473, 0.465, and 0.494, p=0.0007, 0.0014, and 0.0008, respectively; max IMT: ρ=0.558, 0.443, and 0.514, p=0.0001, 0.0024, and 0.0004, respectively). With increasing PVH grades, relative diastolic flow velocity, V_d/V_s, tends to decrease. In particular, état criblé showed a significant negative association with V_d/V_s ($\rho=-0.418$, p=0.0038; Figs. 1–3).

Determinant factors for PVH, DSWMH, and état criblé were analyzed by a stepwise regression analysis with age, PP, TC, mean IMT and V_d/V_s as independent variables. Age was independently associated with PVH, DSWMH and état criblé (the partial correlation coefficients were 0.606, 0.554 and 0.593; $p<$ 0.0001, 0.0001 and 0.0001, respectively).

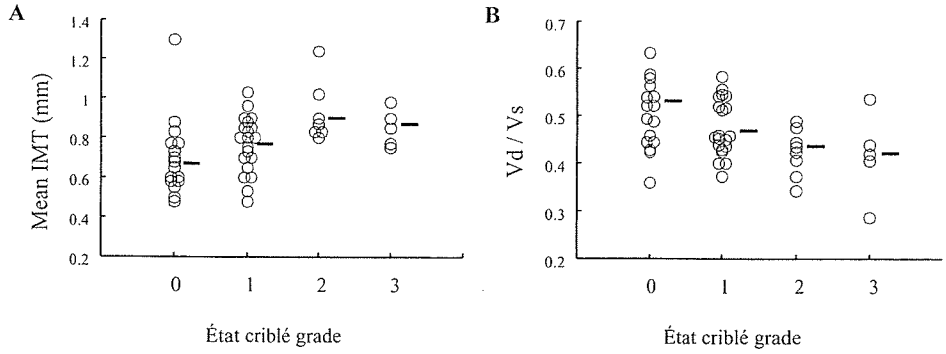

Fig. 3. *The relationship between état criblé grades and IMT (A) and relative diastolic velocity (B). The état criblé grades were positively correlated with IMT and negatively correlated with* V_d/V_s. ▬, *mean values of mean IMT and* V_d/V_s.

Discussion

The advent of brain imaging methods, particularly MRI, has revealed a multitude of focal, patchy, and diffuse signal changes in the cerebrum (*19–21*). There are variable visual rating scales for these lesions, but these scales are not consistent (*21*). In this study, we employed the Japanese Braindock Guidelines based on Fazekas's scale (*16*) in order to classify the incidence of PVH, DSWMH, and état criblé. The pathogenesis of cerebral white matter abnormalities, PVH, and DSWMH are sometimes described as "leukoaraiosis," and it has been reported that these features are the result of ischemic injury to the brain (*22*). Silent, small hyperintense foci of the basal ganglia and thalamus are also frequently noted on MRI. These foci are lacuna infarctions and perivascular spaces (état criblé). Lacuna and état criblé are distinguished by their size and margin type (irregular or smooth) (*23*). We determined that état criblé have the following features on MRI: high-intensity T_2-weighted images, smooth margins, and lesions of <3 mm in diameter. It has been reported that état criblé increases with the age and is associated with hypertension. Progressive arteriolosclerosis of the perforating arteries is assumed with a histopathology of état criblé, which renders cerebral tissue compressed and atrophied (*8*).

In this study, we evaluated white and deep gray matter lesions using MRI in hypertensive patients without diabetes, impaired glucose tolerance, arrhythmia, or a previous cardiovascular event. We first investigated the relationships between the MRI findings and the following atherosclerotic risk factors: age, PP, body mass index (BMI), TC and smoking. There was a strong correlation between MRI findings and age (Table 3). Previous studies (*4–7*, *24–28*) have demonstrated that age and hypertension were strongly and independently correlated with white matter lesions and état criblé. Similar to previous studies, the present study also demonstrated that age was positively related to the severity of hyperintensity changes in both the white matter and deep gray matter.

In addition, we found a positive correlation between PVH and PP. As the mechanism of PP increase, decreases in Windkessel function and increases in arterial stiffness appeared to be involved (*29*, *30*). Arterial stiffness increases SBP and reduces DBP. Increases in PP lead to decreases in diastolic blood flow to the brain (*31*, *32*). The Rotterdam Scan Study (*33*) and the Framingham Heart Study (*34*) also demonstrated that low DBP was a risk for subsequent brain infarction. Drops in DBP and increases in PP are consequences of arterial stiffening, as part of the progression of arteriolosclerosis possibly associated with PVH. In this study, PVH grade was significantly associated with PP, but DSWMH grade was not. The periventricular white matter is an arterial border zone, already marginally perfused under physiologic circumstances, which makes it especially vulnerable under a decrease of cerebral blood flow. In contrast, the subcortical white matter is better vascularized and is not an arterial watershed area (*35*, *36*). Because of this pathophysiological characteristic, PVH may be more susceptible to PP than DSWMH.

Furthermore, we evaluated the relationship between the MRI findings and the carotid US parameters. The Cardiovascular Health Study previously demonstrated strong relationships between white matter lesions and carotid IMT and stenosis (*37*). Kitamura *et al.* reported that increased IMT is a risk factor for stroke in Japanese elderly men (*38*). In the present study, PVH, DSWMH, and état criblé were positively associated with the IMT. This indicated that severity of PVH, DSWMH, and/or état criblé reflect hypertensive organ damages and might be high risk for further stroke.

We previously evaluated changes in the hemodynamics of the CCA using Doppler US (*39*, *40*). The relative diastolic flow (V_d/V_s) of the CCA in hypertensive patients with insulin resistance (IR) or left ventricular hypertrophy (LVH) is lower than that of normotensive subjects (*12*, *41*). The V_d/V_s represent the resistance of the peripheral arteries. In the current study, V_d/V_s was more strongly associated with état criblé than PVH. The white matter adjacent to the lateral ventricle walls, which is called a "watershed zone," receives from ventriculofugal vessels arising from the subependymal arteries. Poor

vascularity in these parts easily causes hypoxic/ischemic injury due to the low perfusion. Pathogenesis of PVH is due to these anatomical characteristics. On the other hand, état criblé is characterized by vascular ectasia and dilated perivascular spaces, and reflects shrinkage or atrophy of the brain parenchyma around blood vessels (*35*). The état criblé may reflect the peripheral vascular resistance more strongly than PVH depending on the difference in the pathophysiological characteristics between them.

There were some limitations in this study. First, the study population was relatively small, because we excluded the patients with congestive heart failure, previous myocardial infarction, atrial fibrillation, diabetes mellitus, impaired glucose tolerance, chronic renal failure, and history of stroke. Second, we did not evaluate the maximum IMT of the internal carotid artery (ICA). In their cohort study, Kitamura *et al.* reported that the combination of CCA and ICA wall thickness was a better predictor of the risk of stroke than was CCA wall thickness alone (*38*). Further study is needed to clarify the relationship between the max IMT of ICA and asymptomatic MRI findings.

In conclusion, in patients with EHT, asymptomatic white matter hyperintensity and deep gray matter lesions were related to the severity of carotid atherosclerosis, *i.e.*, the IMT. The blood flow velocity, as estimated by the relative diastolic blood flow in the CCA, was decreased in patients with severe état criblé. Carotid structure and hemodynamics are potentially related to asymptomatic lesions in the cerebrum and may be predictors of future cerebral vascular event in patients with EHT.

References

1. Hachinski VC: Stroke and hypertension and its prevention. *Am J Hypertens* 1991; **4**: S118–S120.
2. Miyao S, Takano A, Teramoto J, Takahashi A: Leukoaraiosis in relation to prognosis for patients with lacunar infarction. *Stroke* 1992; **23**: 1434–1438.
3. van Swieten JC, Kappelle LJ, Algra A, van Latum JC, Koudstaal PJ, van Gijn J, for the Dutch TIA Trial Study Group: Hypodensity of the cerebral white matter in patients with transient ischemic attack or minor stroke: influence on the rate of subsequent stroke. *Ann Neurol* 1992; **32**: 177–183.
4. Jørgensen HS, Nakayama H, Raaschou HO, Gam J, Olsen TS: Silent infarction in acute stroke patients. Prevalence, localization, risk factors, and clinical significance: the Copenhagen Stroke Study. *Stroke* 1994; **25**: 97–104.
5. Davis PH, Clarke WR, Bendixen BH, Adams HP Jr, Woolson RF, Culebras A, the TOAST Investigators: Silent cerebral infarction in patients enrolled in the TOAST study. *Neurology* 1996; **46**: 942–948.
6. Boon A, Lodder J, van Raak LH, Kessels F: Silent brain infarcts in 755 consecutive patients with a first-ever supratentorial ischemic stroke: relationship with index-stroke subtype, vascular risk factors, and mortality. *Stroke* 1994; **25**: 2384–2390.
7. Kobayashi S, Okada K, Koide H, Bokura H, Yamaguchi S: Subcortical silent brain infarction as a risk factor for clinical stroke. *Stroke* 1997; **28**: 1932–1939.
8. Awad IA, Johnson PC, Spetzler RF, Hodak LA: Incidental subcortical lesions identified on magnetic resonance imaging in the elderly. II. Postmortem pathological correlations. *Stroke* 1986; **17**: 1090–1097.
9. O'Leary DH, Polak JF, Kronmal RA, Manolio TA, Burke GL, Wolfson SK Jr, for the Cardiovascular Health Study Collaborative Research Group: Carotid-artery intima and media thickness as a risk factor for myocardial infarction and stroke in older adults. *N Engl J Med* 1999; **340**: 14–22.
10. Chambless LE, Folsom AR, Clegg LX, *et al*: Carotid wall thickness is predictive of incident clinical stroke. The Atherosclerosis Risk in Communities (ARIC) Study. *Am J Epidemiol* 2000; **151**: 478–487.
11. Hollander M, Bots ML, Iglesias del Sol A, *et al*: Carotid plaques increase the risk of stroke and subtypes of cerebral infarction in asymptomatic elderly. The Rotterdam Study. *Circulation* 2002; **105**: 2872–2877.
12. Jiang Y, Kohara K, Hiwada K: Alteration of carotid circulation in essential hypertensive patients with left ventricular hypertrophy. *J Hum Hypertens* 1998; **12**: 173–179.
13. Jiang Y, Kohara K, Hiwada K: Low wall shear stress in carotid arteries in subjects with left ventricular hypertrophy. *Am J Hypertens* 2000; **13**: 892–898.
14. Simons PCG, Algra A, Michiel L, Bots ML, Grobbee DE, van der Graaf Y, for the SMART Study Group: Common carotid intima-media thickness and arterial stiffness. Indicators of cardiovascular risk in high-risk patients. The SMART Study (Second Manifestations of ARTerial disease). *Circulation* 1999; **100**: 951–957.
15. Hashi K, Kobayashi S, Saitou I, *et al*: Braindock Guideline. Sapporo, Japanese Society for Detection of Asymptomatic Brain Disease, 2003, pp 49–53.
16. Fazekas F, Chawluk JB, Alavi A, Hurtig HI, Zimmerman RA: MR signal abnormalities at 1.5 T in Alzheimer's dementia and normal aging. *Am J Roentgenol* 1987; **149**: 351–356.
17. Uehara T, Tabuchi M, Mori E: Risk factors for silent cerebral infarcts in subcortical white matter and basal ganglia. *Stroke* 1999; **30**: 378–382.
18. National Institute of Neurological Disorders and Stroke: Classification of cerebrovascular disease III. *Stroke* 1990; **21**: 637–676.
19. Shimada K, Kawamoto A, Matsubayashi K, Nishinaga M, Kimura S, Ozawa T: Diurnal blood pressure variations and silent cerebrovascular damage in elderly patients with hypertension. *J Hypertens* 1992; **10**: 875–878.
20. Awad IA, Spetzler RF, Hodak JA, Awad CA, Carey R: Incidental subcortical lesions identified on magnetic resonance imaging in the elderly. I. Correlation with age and cerebrovascular risk factors. *Stroke* 1986; **17**: 1084–1089.
21. Mäntylä R, Erkinjuntti T, Salonen O, *et al*: Variable agreement between visual rating scales for white matter hyperintensities on MRI. Comparison of 13 rating scales in a poststroke cohort. *Stroke* 1997; **28**: 1614–1623.
22. Ginsberg MD, Hedley-Whyte ET, Richardson EP Jr: Hypoxic-ischemic leukoencephalopathy in man. *Arch Neurol* 1976; **33**: 5–14.

23. Takao M, Koto A, Tanahashi N, Fukuuchi Y, Takagi M, Morinaga S: Pathologic findings of silent, small hyperintense foci in the basal ganglia and thalamus on MRI. *Neurology* 1999; **52**: 666–668.
24. Bernick C, Kuller L, Dulberg C, *et al*, for the Cardiovascular Health Study Collaborative Research Group: Silent MRI infarcts and the risk of future stroke. The cardiovascular health study. *Neurology* 2001; **57**: 1222–1229.
25. Shintani S, Shiigai T, Arinami T: Silent lacunar infarction on magnetic resonance imaging (MRI): risk factors. *J Neurol Sci* 1998; **160**: 82–86.
26. Yamamoto Y, Akiguchi I, Oiwa K, Hayashi M, Ohara T, Ozasa K: The relationship between 24-hour blood pressure readings, subcortical ischemic lesions and vascular dementia. *Cerebrovasc Dis* 2005; **19**: 302–308.
27. Shimada K, Kawamoto A, Matsubayashi K, Ozawa T: Silent cerebrovascular disease in the elderly. *Hypertension* 1990; **16**: 692–699.
28. Eguchi K, Kario K, Hoshide S, *et al*: Smoking is associated with silent cerebrovascular disease in a high-risk Japanese community-dwelling population. *Hypertens Res* 2004; **27**: 747–754.
29. Smulyan H, Safar ME: The diastolic blood pressure in systolic hypertension. *Ann Intern Med* 2000; **132**: 233–237.
30. London GE, Guerin AP: Influence of arterial pulse and reflected waves on blood pressure and cardiac function. *Am Heart J* 1999; **138**: S220–S224.
31. Eguchi K, Kario K, Hoshide S, *et al*: Greater change of orthostatic blood pressure is related to silent cerebral infarct and cardiac overload in hypertensive subjects. *Hypertens Res* 2004; **27**: 147–156.
32. Ogihara T, Hiwada K, Morimoto S, *et al*: Guidelines for treatment of hypertension in the elderly—2002 revised version—. *Hypertens Res* 2003; **26**: 1–36.
33. Vermeer SE, Hollander M, van Dijk EJ, Hofman A, Koudstaal PJ, Breteler MMB: Silent brain infarcts and white matter lesions increase stroke risk in the general population. The Rotterdam Scan Study. *Stroke* 2003; **34**: 1126–1129.
34. Franklin SS, Larson MG, Khan SA, *et al*: Does the relation of blood pressure to coronary heart disease risk change with aging? The Framingham Heart Study. *Circulation* 2001; **103**: 1245–1249.
35. Leeuw F-E, Groot JC, Oudkerk JC, *et al*: Atrial fibrillation and the risk of cerebral white matter lesions. *Neurology* 2000; **54**: 1795–1800.
36. Pantoni L, Garcia JH: Pathogenesis of leukoaraiosis. *Stroke* 1997; **28**: 652–659.
37. Manolio TA, Burke GL, O'Leary DH, *et al*, for the CHS Collaborative Research Group: Relationships of cerebral MRI findings to ultrasonographic carotid atherosclerosis in older adults. The Cardiovascular Health Study. *Arterioscler Thromb Vasc Biol* 1999; **19**: 356–365.
38. Kitamura A, Iso H, Imano H, *et al*: Carotid intima-media thickness and plaque characteristics as a risk factor for stroke in Japanese elderly men. *Stroke* 2004; **35**: 2788–2794.
39. Watanabe S, Okura T, Liu J, *et al*: Serum cystatin C level is a marker of end-organ damage in patients with essential hypertension. *Hypertens Res* 2003; **26**: 895–899.
40. Okura T, Watanabe S, Miyoshi K, Fukuoka T, Higaki J: Intrarenal and carotid hemodynamics in patients with essential hypertension. *Am J Hypertens* 2004; **17**: 240–244.
41. Watanabe S, Okura T, Kitami Y, Hiwada K: Carotid hemodynamic alterations in hypertensive patients with insulin resistance. *Am J Hypertens* 2002; **15**: 851–856.

Journal of Human Hypertension (2005) 19, 787–791

www.nature.com/jhh

ORIGINAL ARTICLE

Association between carotid haemodynamics and inflammation in patients with essential hypertension

S Manabe, T Okura, S Watanabe and J Higaki
The Second Department of Internal Medicine, Ehime University School of Medicine, Toon City, Ehime, Japan

Previous studies have shown that high blood pressure causes chronic inflammation. Hypertensive patients are reported to have high-circulating levels of proinflammatory cytokines such as interleukin-6 (IL-6) and high sensitive C-reactive protein (hs-CRP). The pulsatility index (PI) and resistive index (RI) are used as markers of peripheral vascular resistance. In the present study, we evaluated the relationship between carotid haemodynamics and the proinflammatory cytokines, IL-6 and hs-CRP. In all, 41 patients with essential hypertension participated. The intima-media thickness (IMT), peak systolic velocity (pVs), peak diastolic velocity (pVd) and mean velocity (mV) in the common carotid artery were measured using ultrasound Doppler flow methods, and PI [(pVs−pVd)/mV] and RI [(pVs−pVd)/pVs] were calculated. Serum IL-6 and hs-CRP concentrations were measured by an enzyme-linked immunosorbent assay. IMT was positively correlated with age and pulse pressure. Both PI and RI were positively correlated with pulse pressure, IL-6 and hs-CRP. A multiple regression analysis revealed that PI and RI were independently associated with hs-CRP. These results suggested that carotid haemodynamic parameters such as PI and RI are associated with atherosclerosis and inflammation in hypertensive patients.
Journal of Human Hypertension (2005) **19,** 787–791.
doi:10.1038/sj.jhh.1001898; published online 23 June 2005

Keywords: pulsatility index; resistive index; intima-media thickness; interleukin-6; high sensitive CRP

Introduction

Inflammation may contribute to the initiation and progression of atherosclerosis.[1,2] High blood pressure may promote vascular oxidative stress and exert a proinflammatory influence on the arterial wall through redox-sensitive mechanisms.[3] Indeed, hypertensive patients who were free from any other important medical conditions were reported to have high circulating levels of proinflammatory cytokines such as tumor necrosis factor-α (TNF-α), interleukin-6 (IL-6),[4] and C-reactive protein (CRP).[5,6] These cytokines may cause inflammation of the endothelium,[7,8] which can cause further damage to the endothelium[9] and the elevation of blood pressure. One of the most useful factors for estimating the inflammatory response and the risk for vascular events is high sensitive CRP (hs-CRP). The hepatic production of hs-CRP is regulated by the proinflammatory cytokines TNF-α, IL-1β and IL-6. IL-6 is a pleiotropic cytokine and central mediator of the acute-phase response and has a broad range of effects on diverse immune cells such as vascular endothelial cells, smooth muscle cells and leucocytes.[10] IL-6[11,12] and CRP[13–15] are also expressed in human atherosclerotic lesions.

B-mode ultrasound imaging of the common carotid artery (CCA) has been developed and standardized for *in vivo* evaluation of early atherosclerotic lesions.[16,17] Hypertensive patients have a greater intima-media thickness (IMT)[18] and a higher prevalence of plaques in the CCA than normotensive individuals. These structural alterations of the CCA are related to cardiovascular complications[19] and can lead to cerebrovascular events, which strongly suggests that early detection of these alterations is clinically important for the management of hypertensive patients.

Recently, Doppler ultrasound has been used as a method to evaluate not only significant stenosis or plaque formation but also haemodynamic alterations in the CCA in hypertensive patients.[20] In the present study, we evaluated the relationship between serum proinflammatory markers and atherosclerosis as estimated by IMT and carotid haemodynamics in patients with essential hypertension.

Correspondence: T Okura, The Second Department of Internal Medicine, Ehime University School of Medicine, Toon City, Ehime, 791-0295 Japan.
E-mail: Okura@m.ehime-u.ac.jp
Received 1 April 2005; revised 28 April 2005; accepted 29 April 2005; published online 23 June 2005

Methods

Patients

Patients with essential hypertension participated in this study. They were recruited from consecutive cases admitted to Ehime University Hospital from July 2001 to January 2004. Hypertension was defined as a systolic blood pressure (SBP) >140 mmHg or a diastolic blood pressure (DBP) >90 mmHg measured three times in the sitting position using a brachial sphygmomanometer. Patients with diabetes mellitus, thyroid disease, coronary artery disease, previous stroke, renal dysfunction (serum creatinine >1.2 mg/dl), peripheral vascular disease or who were suspected of having acute inflammatory diseases or malignant disease were excluded. All patients were untreated or had discontinued treatment at least 2 weeks before the investigation. Informed consent to the procedures was obtained from each patient.

Measurement of proinflammatory cytokines

Serum hs-CRP and IL-6 were measured by enzyme-linked immunosorbent assay kits (Alpha Diagnostic, San Antonio, TX, USA; PIERCE Endogen, Rockford IL, USA, respectively). Measurements of serum creatinine, total cholesterol, high-density lipoprotein (HDL)-cholesterol and triglyceride were carried out using an automatic analyzer (model TBA-60S; Toshiba Inc., Tokyo, Japan).

Ultrasound analysis of the CCA

Carotid arteries were evaluated using an SSD-2000 (Aloka Co., Tokyo, Japan) with a 7.5 MHz probe as previously described.[21] After the patient had rested for at least 10 min in the supine position with the neck in slight hyperextension, we examined an optimal visualization of the CCA, carotid bulb and extra-cranial internal and external carotid arteries on both sides. The IMT of the far wall was measured in the CCA at both 1 and 2 cm proximal to the bulb from the anterior, lateral and posterior approaches, and then averaged to obtain the mean IMT. Measurements were never taken at the level of discrete plaque. Doppler evaluation was performed on the right CCA in the anterior projection. With the guidance of colour flow mapping, the sample volume was located at the middle of the arterial cavity. Peak systolic velocity (pVs) and peak diastolic velocity (pVd) were obtained from the flow velocity curve. Flow velocity–time integrals of systolic and diastolic phases were computed automatically by electronic integration of the instantaneous flow velocity curves to calculate the mean velocity (mV). Further pulsatility and resistive indexes were calculated from the Doppler spectrum as follows:

$$\text{Pulsatility index (PI)} = (\text{pVs} - \text{pVd})/\text{mV}$$

$$\text{Resistive index (RI)} = (\text{pVs} - \text{pVd})/\text{pVs}$$

Statistical analysis

The results are expressed as mean±s.d. Pearson's correlation coefficient was used to test the association between two kinds of parameters. A multiple regression analysis was applied to the determinant factor of IL-6 and hs-CRP. A probability of <0.05 was considered significant.

Results

Characteristics of the study subjects

A total of 41 patients with essential hypertension were enrolled in this study. Clinical characteristics of the study participants are shown in Table 1.

Proinflammatoly cytokine and carotid IMT and haemodynamics

Table 2 shows the mean values for IL-6, hs-CRP and carotid IMT and haemodynamics.

Association between IL-6, hs-CRP and carotid haemodynamics

IMT was correlated positively with age ($r=0.710$, $P<0.001$) and pulse pressure ($r=0.436$, $P=0.004$).

Table 1 Clinical characteristics of the participants (mean±s.d.)

Number (male/female)	*41 (20/21)*
Age (years)	62±12
BMI (kg/m²)	24.4±2.9
SBP (mmHg)	161±19
DBP (mmHg)	91±13
Mean blood pressure (mmHg)	114±13
Pulse pressure (mmHg)	70±17
Pulse rate (/min)	72±12
Total cholesterol (mg/dl)	207±26
Triglyceride (mg/dl)	166±112
HDL cholesterol (mg/dl)	57±16
Serum creatinine (mg/dl)	0.8±0.3
Glucose (mg/dl)	116±59
HbA1c (%)	5.5±0.9

Table 2 Carotid haemodynamics and proinflammatory markers (mean±s.d.)

Pulsatility index (PI)	1.27±0.405
Resistive index (RI)	0.535±0.082
Mean intima-media thickness (mIMT) (mm)	0.807±0.148
Interleukin-6 (IL-6) (pg/ml)	9.22±1.50
C-reactive protein (CRP) (ng/ml)	1429±0.148

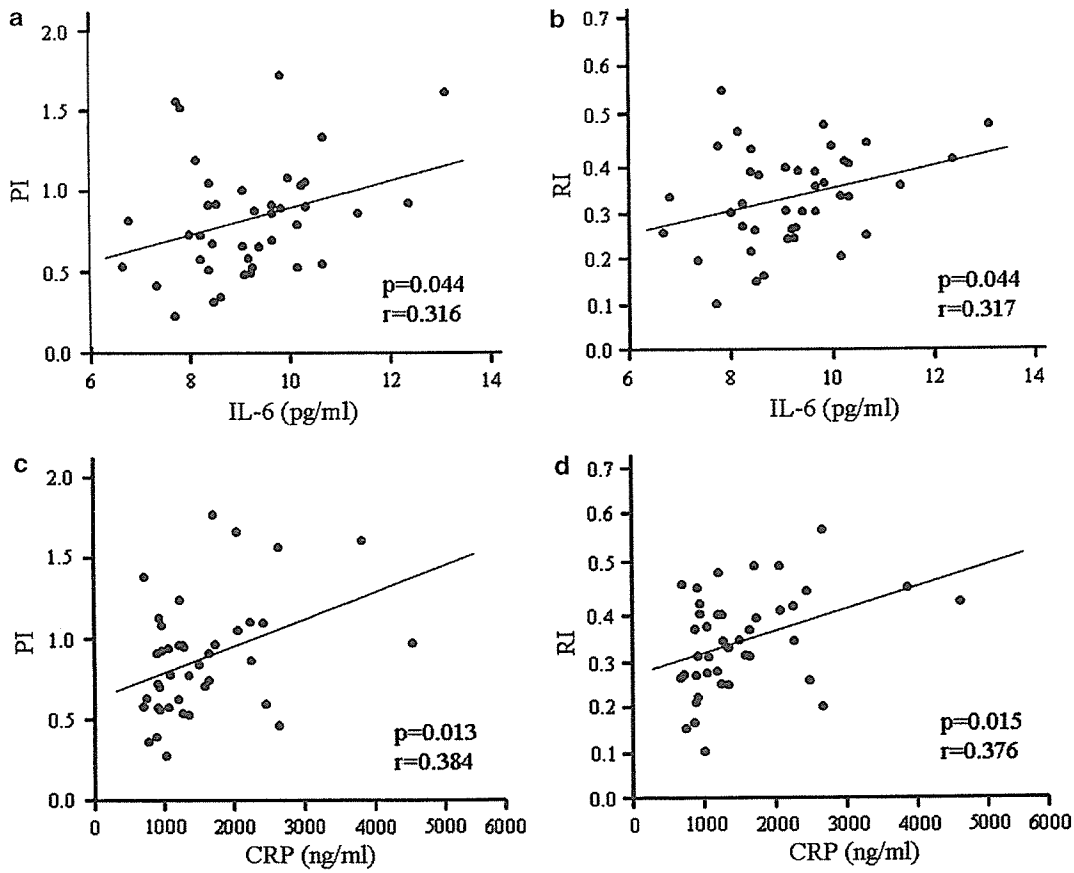

Figure 1 Correlation between carotid haemodynamics and inflammatory parameters. (a) relationship between pulsatility index and IL-6, (b) relationship between resistive index and IL-6, (c) relationship between pulsatility index and hs-CRP, (d) relationship between resistive index and hs-CRP. IL-6 = interleukin-6, hs-CRP = high sensitive-C reactive protein.

Both PI and RI were positively correlated with pulse pressure ($r=0.336$, $P=0.032$, and $r=0.354$, $P=0.023$, respectively), IL-6 ($r=0.316$, $P=0.044$, and $r=0.317$, $P=0.044$, respectively) (Figure 1a and b) and hs-CRP ($r=0.384$, $P=0.013$, and $r=0.376$, $P=0.015$, respectively) (Figure 1c and d). IMT was associated with PI ($r=0.311$, $P=0.048$), but not with RI ($r=0.268$, $P=0.068$), IL-6 ($r=0.170$. $P=0.288$) and hs-CRP ($r=0.103$, $P=0.518$). A multiple regression analysis was performed to identify the independent determinant factor for PI, RI and IMT with age, body mass index (BMI), mean blood pressure, total cholesterol, IL-6 and hs-CRP as independent variables. Table 3 shows that both PI and RI were independently associated with hs-CRP (with partial correlation coefficients of 0.430 and 0.430, $P=0.010$ and $P=0.010$, respectively) and IMT was independently associated with age (with partial correlation coefficients of 0.721, $P=<0.001$).

Discussion

The present study is the first to demonstrate that carotid haemodynamic alteration as expressed in both PI and RI was associated with inflammatory markers, serum IL-6 and hs-CRP in patients with essential hypertension.

A high index of PI and RI is associated with a large difference in velocity between the systolic and diastolic phases as detected by a pulse–wave Doppler ultrasound. This difference in flow velocities reflects downstream resistance, which could at least in part depend on the degree of peripheral arterial stiffness. Originally, PI and RI were introduced by Gosling *et al*[22] and Pourcelot *et al*[23] respectively, to detect peripheral vascular disease. Today, PI and RI are mainly measured in the renal arteries to evaluate the severity of renal failure and renal artery stenosis. Recently, Pontremoli *et al*[24] reported that in essential hypertensive patients, increased renal PI and RI are associated with hypertensive end-organ damage, such as carotid IMT and cardiac hypertrophy, as well as renal function. Previously, we measured the renal and carotid flow in essential hypertension and showed that both approaches are useful for the evaluation of arterial stiffness.[25] Nakatou *et al*[26] measured carotid PI and RI in Type II diabetic patients and reported the usefulness of the carotid PI and RI as well as IMT in estimating the risk of previous cerebral infarction. In the present study, we are able to show that the

Table 3 Multiple regression analyses for pulsatility index (PI), resistive index (RI) and intima-media thickness (IMT)

	Age	*mBP*	*TC*	*BMI*	*IL-6*	*CRP*
PI	0.159 ($P=0.310$)	0.090 ($P=0.560$)	0.048 ($P=0.757$)	0.197 ($P=0.206$)	0.203 ($P=0.190$)	0.430* ($P=0.010$)
RI	0.168 ($P=0.285$)	0.136 ($P=0.382$)	0.117 ($P=0.382$)	0.162 ($P=0.296$)	0.205 ($P=0.184$)	0.430* ($P=0.010$)
mIMT	0.721* ($P<0.001$)	−0.081 ($P=0.497$)	0.178 ($P=0.139$)	0.176 ($P=0.145$)	0.016 ($P=0.892$)	0.030 ($P=0.794$)

mBP = mean blood pressure, TC = total cholesterol, BMI = body mass index, IL-6 = interleukin-6, CRP = C-reactive protein. * = $P<0.05$.

carotid haemodynamics (both PI and RI) are correlated with pulse pressure, indicating that PI and RI are the indices of arterial stiffness, as found in our previous studies. IMT is another useful and established sonographic marker for atherosclerosis, and with increases in IMT being related to future cardiovascular events.[27,28] In the present study, we could show that IMT was correlated with age and pulse pressure, but not with IL-6 or hs-CRP. However, both PI and RI are associated with IL-6 and hs-CRP. The difference in results between the carotid haemodynamic parameters and IMT might be time related. Both PI and RI might refer to the present status of the atherosclerotic change, as do inflammatory markers such as IL-6 and hs-CRP. On the other hand, IMT is the result of the integration of atherosclerotic stimulation that occurs over a long time period, such as hypertension. In this regard, carotid haemodynamic change is a useful atherosclerotic marker that provides a different viewpoint on atherosclerosis than IMT.

It is now well established that inflammation plays a central role in the development of atherosclerosis and its complications.[1,9] Inflammatory markers such as CRP and IL-6 not only participate in lesion formation but also in the plaque architecture that favours rupture.[7] A number of studies have shown that increased blood pressure has an important influence on elevated levels of circulating IL-6[4] and hs-CRP.[5,6,17] IL-6 and hs-CRP were also suggested to be strong independent predictors of the risk of future cardiovascular events.[28–34] The present study, which shows a relationship between carotid haemodynamic change and inflammatory markers, indicates that PI and RI could also help to predict further cardiovascular events.

As shown in Table 3, hs-CRP but not IL-6 is an independent determinant factor for PI and RI. This result suggests that carotid haemodynamics is related to the level of systemic inflammation, and the inflammatory marker hs-CRP may be more sensitive than IL-6. One limitation of this study is the small number of subjects enrolled. The pathogenesis of low-grade inflammation is different between patients with essential hypertension and patients with diabetes mellitus, thyroid disease, coronary artery disease, previous stroke, peripheral or vascular disease. For this reason, we excluded these patients with hypertension from this study. It is necessary to confirm our findings by studies with large number of patients. Furthermore, studies that clarify the relationship between carotid haemodynamics and other inflammatory cytokines and markers such as TNF-α and IL-1β, as well as IL-6 and hs-CRP are needed.

In conclusion, carotid haemodynamics as expressed by both PI and RI are associated with pulse pressure and the inflammatory markers IL-6 and hs-CRP. Furthermore, hs-CRP is an independent determinant factor for PI and RI. These results indicate that carotid haemodynamic alteration is a useful marker of atherosclerosis as an inflammatory disease. Further prospective study is needed to establish carotid haemodynamics; PI and RI are reliable predictors of further cardiovascular events in essential hypertensive patients.

(a) What is known on this topic

1. Hypertensive patients have high circulating levels of proinflammatory cytokines such as interleukin-6 (IL-6) and high sensitive C-reactive protein (hs-CRP).
2. Both IL-6 and hs-CRP are independent risk factors of cardiovascular disease.
3. Hypertensive patients have a greater intima-media thickness (IMT), and a higher pulsatility index (PI) and resistive index (RI) in the common carotid artery.

(b) What this study adds

1. Carotid haemodynamics, PI and RI, are correlated with IL-6 and hs-CRP.
2. Hs-CRP is an independent determinant factor for PI and RI.

References

1 Ross R. Atherosclerosis: an inflammatory disease. *N Engl J Med* 1999; **340**: 115–126.
2 Libby P. Inflammation in atherosclerosis. *Nature* 2002; **420**: 868–874.
3 Lacy F, O'Connor DT, Schmid-Schonbein GW. Plasma hydrogen peroxide production in hypertensives and normotensive subjects at genetic risk of hypertension. *J Hypertens* 1998; **16**: 291–303.
4 Chae CU, Lee RT, Rifai N, Ridker PM. Blood pressure and inflammation in apparently healthy men. *Hypertension* 2002; **38**: 399–403.
5 Bautista LE *et al.* Is C-reactive protein an independent risk factor for essential hypertension? *J Hypertens* 2001; **19**: 857–861.
6 Abramson JL, Weintraub WS, Vaccarino V. Association between pulse pressure and C-reactive protein among

apparently healthy US adults. *Hypertension* 2002; **39**: 197–202.
7 Blake GJ, Ridker PM. Novel clinical markers of vascular wall inflammation. *Circ Res* 2001; **89**: 763–771.
8 Gabay C, Kushner I. Acute-phase proteins and other systemic responses to inflammation. *N Engl J Med* 1999; **340**: 448–454.
9 Rattazzi M *et al.* C-reactive protein and interleukin-6 in vascular disease: culprits or passive bystanders? *J Hypertens* 2003; **21**: 1787–1803.
10 Van Snick J. Interleukin-6 an overview. *Annu Rev Immunol* 1990; **8**: 253–278.
11 Seino Y *et al.* Interleukin 6 gene transcripts are expressed in human atherosclerotic lesions. *Cytokine* 1994; **6**: 87–91.
12 Rus HG, Vlaicu R, Niculescu F. Interleukin-6 and interleukin-8 protein and gene expression in human arterial atherosclerotic wall. *Atherosclerosis* 1996; **127**: 263–271.
13 Reynolds GD, Vance RP. C-reactive protein immunohistochemical localization in normal and atherosclerotic human aortas. *Arch Pathol Lab Med* 1987; **111**: 265–269.
14 Hatanaka K *et al.* Immunohistochemical localization of C-reactive protein-binding sites in human atherosclerotic aortic lesions by a modified streptavidin-biotin-staining method. *Pathol Int* 1995; **45**: 635–641.
15 Zhang YX, Cliff WJ, Schoefl GI, Higgins G. Coronary C-reactive protein distribution: its relation to development of atherosclerosis. *Atherosclerosis* 1999; **145**: 375–379.
16 Pignoli P *et al.* Intimal plus medial thickness of the arterial wall: a direct measurement with ultrasound imaging. *Circulation* 1986; **74**: 1399–1406.
17 Pignoli P, Longo T. Evaluation of atherosclerosis with B-mode ultrasound imaging. *J Nucl Med Allied Sci* 1988; **32**: 166–173.
18 Casiglia E, Palatini P, Da Ros S, Pagliara V. Effect of blood pressure and physical activity on carotid artery intima-media thickness in stage 1 hypertensives and controls. *Am J Hypertens* 2000; **13**: 1256–1262.
19 Takiuchi S *et al.* Diagnostic value of carotid intima-media thickness and plaque score for predicting target organ damage in patients with essential hypertension. *J Hum Hypertens* 2004; **18**: 17–23.
20 Frauchiger B *et al.* Comparison of carotid arterial resistive insices with intima-media thickness as sonographic markers of atherosclerosis. *Stroke* 2001; **32**: 836–841.
21 Watanabe S, Okura T, Kitami Y, Hiwada K. Carotid hemodynamic alterations in hypertensive patients with insulin resistance. *Am J Hypertens* 2002; **15**: 851–856.
22 Gosling RG *et al.* The quantitative analysis of occlusive peripheral arterial disease by a non-intrusive ultrasonic technique. *Angiology* 1971; **22**: 52–55.
23 Poircelot L. Indications of Doppler's ultrasonography in the study of peripheral vessels. *Rev Prat* 1975; **25**: 4671–4680.
24 Pontremoli R *et al.* Increased renal resistive index in patients with essential hypertension: a marker of target organ damage. *Nephrol Dial Transplant* 1999; **14**: 360–365.
25 Okura T *et al.* Intrarenal and carotid hemodynamics in patients with essential hypertension. *Am J Hypertens* 2004; **17**: 240–244.
26 Nakatou T, Nakata K, Nakamura A, Itoshima T. Carotid hemodynamic parameters as risk factors for cerebral infarction in Type 2 diabetic patients. *Diabet Med* 2004; **21**: 223–229.
27 Ebrahim S *et al.* Carotid plaque, intima media thickness cardiovascular risk factors, and prevalent cadiovascular disease in men and women. *Stroke* 1999; **30**: 841–850.
28 Barth JD. An update on carotid ultrasound measurement of intima-media thickness. *Am J Cardiol* 2002; **89**(suppl): 32B–39B.
29 Sung KC *et al.* High sensitivity C-reactive protein as an independent risk factor for essential hypertension. *Am J Hypertens* 2003; **16**: 429–433.
30 Ridker PM. High-sensitivity C-reactive protein and cardiovascular risk: rationale for screening and primary prevention. *Am J Cardiol* 2003; **92**(suppl): 17K–122K.
31 Mendall MA *et al.* C-reactive protein and its relation to cardiovascular risk factors: a population based cross sectional study. *BMJ* 1996; **312**: 1061–1065.
32 Rohde LED, Hennekens CH, Ridker PM. Survey of C-reactive protein and cardiovascular risk factors in apparently healthy men. *Am J Cardiol* 1999; **84**: 1018–1022.
33 Yudkin JS, Kumari M, Humphries SE, Mohamed-Ali V. Inflammation, obesity, stress and coronary heart disease: is interleukin-6 the link? *Atherosclerosis* 2000; **148**: 209–214.
34 Choi H, Cho DH, Shin HH, Park JB. Association of high sensitivity C-reactive protein with coronary heart disease prediction, but not with carotid atherosclerosis, in patients with hypertension. *Circ J* 2004; **68**: 297–303.

Effects of Angiotensin II Receptor Blockade with Valsartan on Pro-Inflammatory Cytokines in Patients with Essential Hypertension

Seiko Manabe, MD, Takafumi Okura, MD, Sanae Watanabe, MD, Tomikazu Fukuoka, MD, and Jitsuo Higaki, MD

Abstract: Chronic inflammation is common in hypertension and acts as an independent determinant of arterial blood pressure. Hypertensive patients are reported to have high circulating levels of pro-inflammatory cytokines such as tumor necrosis factor-α (TNF-α), interleukin-6 (IL-6), and C-reactive protein (CRP). Recently, angiotensin II receptor blockers (ARBs) have been shown to possess benefits in addition to their ability to lower blood pressure, including anti-inflammatory and antioxidative properties within the vasculature. We evaluated the effects of the angiotensin II receptor blocker, valsartan, on these inflammatory cytokines. Thirty-nine patients with essential hypertension participated. These subjects received valsartan, 40 to 80 mg/day. Serum TNF-α, IL-6, CRP, and serum amyloid A (SAA) were measured before and after 3 months of treatment with valsartan. Valsartan significantly decreased systolic and diastolic blood pressure (160 ± 16/92 ± 11 mm Hg to 147 ± 21/84 ± 11 mm Hg, $P = 0.001/P = 0.001$, respectively). Serum TNF-α (9.1 ± 8.6 pg/mL to 6.1 ± 1.0 pg/mL, $P = 0.006$) and IL-6 (9.3 ± 1.7 pg/mL to 8.9 ± 1.4 pg/mL, $P = 0.005$) were significantly reduced after treatment with valsartan. However, C-reactive protein and serum amyloid A did not change. The angiotensin II receptor blocker, valsartan, may inhibit the development of atherosclerosis by lowering serum pro-inflammatory cytokines.

Key Words: C-reactive protein, inflammation, interleukin-6, serum amyloid A, tumor necrosis factor-α

(*J Cardiovasc Pharmacol*™ 2005;46:735–739)

Chronic inflammation is a common link between cardiovascular risk factors and hypertension and acts as an independent determinant of arterial blood pressure. High blood pressure may promote vascular oxidative stress and exerts a pro-inflammatory influence on the arterial wall through redox-sensitive mechanisms that are regulated by angiotensin II.[1] Indeed, hypertensive patients without any other important medical conditions were reported to have high circulating levels of pro-inflammatory risk factors such as tumor necrosis factor-α (TNF-α), interleukin-6 (IL-6),[2,3] and serum C-reactive protein (CRP).[4] These cytokines may cause inflammation of the endothelium,[5] which can cause further damage to the endothelium[6] and further elevation of blood pressure. TNF-α,[7] IL-6,[8] and CRP[9] are also expressed in human atherosclerotic lesions. One of the most useful factors for estimating the inflammatory response and the risk for vascular events is high sensitivity-CRP (hs-CRP). The hepatic production of CRP is regulated by the pro-inflammatory cytokines, TNF-α, IL-1β, and IL-6. IL-6 is a pleiotropic cytokine and the central mediator of the acute-phase response, and has a broad range of effects on diverse immune cells such as vascular endothelial cells, smooth muscle cells, and leukocytes. TNF-α induces the production of IL-6 and the adherence of leukocytes to the endothelium. Furthermore, TNF-α is known to influence lipid[10] and glucose metabolism[11] and to be associated with cardiovascular diseases.[12]

Of the many factors implicated in hypertensive vascular disease, angiotensin II appears to be one of the most important. Angiotensin II has significant pro-inflammatory actions in the vascular wall, inducing the production of reactive oxygen species, inflammatory cytokines, and adhesion molecules.[13] Moreover, angiotensin II participates in tissue repair and remodeling by stimulating cell growth and fibrosis. Recently, angiotensin II has been shown to stimulate the production of cytokines such as TNF-α and IL-6 via the angiotensin II type I receptor, which is present on monocytes, macrophages, and vascular smooth muscle cells.[14]

The ability of angiotensin II receptor blockers (ARBs) to reduce mortality and morbidity of cardiovascular diseases has been ascribed not only to blood pressure-lowering activity but also to a number of additional protective effects. ARBs have potentially protective action against left ventricular hypertrophy,[15] endothelial dysfunction,[16] smooth muscle cell growth,[17] and inflammation[18] in the hypertensive patient.

In the present study, we evaluated the anti-inflammatory effect of the ARB, valsartan, in patients with essential hypertension.

METHODS

Patients

Twenty-nine patients with essential hypertension participated in this study. They were recruited from consecutive 45 essential hypertensive patients admitted to Ehime University Hospital. Hypertension was defined as a systolic blood pressure

Received for publication June 7, 2005; accepted August 20, 2005.
From the Second Department of Internal Medicine, National University Corporation, Ehime University, Toon City, Ehime, Japan.
Reprints: Takafumi Okura, The Second Department of Internal Medicine, National University Corporation, Ehime University, Toon City, Ehime, Japan 791-0295.

(SBP) ≧140 mm Hg or a diastolic blood pressure (DBP) ≧90 mm Hg measured 3 times in the sitting position using a brachial sphygmomanometer. Patients ≧80 years of age were excluded. Patients with renal dysfunction (serum creatinine ≧1.2 mg/dL), diabetes mellitus, thyroid disease, or who were suspected of having acute inflammatory diseases or malignant disease were also excluded. All patients were untreated or had discontinued all medications for hypertension at least 2 weeks before the investigation. After pretreatment assessment, each patient received an initial daily dose of 40 mg valsartan. One month later, patients had valsartan titrated up to 80 mg if either their SBP was above 140 mm Hg or their DBP was above 90 mm Hg. Blood samples were evaluated before and after 3 months of treatment with valsartan. The study complied with the ethical rules for human experimentation in the Declaration of Helsinki. All participants gave their informed consent to the procedures at the time of enrollment, especially to discontinue all medications for hypertension at least 2 weeks before the investigation.

Measurement of Inflammatory Cytokines and Markers

Serum TNF-α, IL-6, CRP, and SAA were measured by enzyme-linked immunosorbent assay kits (BIOSOURCE, BioSource, CA; Alpha Diagnostic, San Antonio, TX; PIERCE Endogen, Rockford, IL; AN'ALYZA, TECHNE, MN; respectively). Measurements of serum creatinine, total cholesterol, high-density lipoprotein (HDL)-cholesterol, and triglyceride were carried out using an automatic analyzer (model TBA-60S; Toshiba Inc., Tokyo, Japan).

Statistical Analysis

The results are expressed as the mean ± SD. Pearson's correlation coefficient was used to test the association between two variables. Changes in blood pressure, pulse pressure, pro-inflammatory cytokines, and markers were analyzed by the Wilcoxon matched-pair signed-ranks test. A probability of less than 0.05 was considered significant.

RESULTS

Characteristics of Study Subjects

Twenty-nine patients (16 males and 13 females, mean age 59 ± 14, 30 to 76 years old) with essential hypertension were enrolled in this study. Clinical characteristics of the study participants are shown in Table 1.

Effects of Angiotensin II Receptor Blockers on Blood Pressure and Inflammatory Cytokines and Markers

Table 2 shows the effects of valsartan on blood pressure and inflammatory cytokines and markers. After treatment with valsartan, SBP was reduced from 160 ± 16 mm Hg at baseline to 147 ± 21 mm Hg at 3 months ($P = 0.001$); DPB was also reduced from 92 ± 11 mm Hg at baseline to 84 ± 11 mm Hg ($P = 0.001$) (Figs. 1A and 1B). Pulse pressure was decreased from 67 ± 15 mm Hg at baseline to 62 ± 18 mm Hg at 3 months ($P = 0.030$). There was no significant difference in serum creatinine after treatment. Serum TNF-α and IL-6 were significantly reduced after 3 months of valsartan therapy (9.1 ± 8.6 versus 6.1 ± 1.0 pg/mL, $P = 0.006$; 9.3 ± 1.7 versus 8.9 ± 1.4 pg/mL, $P = 0.005$; respectively) (Figs. 2A and 2B). Serum CRP and SAA levels before and after treatment (1.5 ± 1.0 versus 1.3 ± 0.7 mg/mL, $P = 0.424$; 13.2 ± 5.6 versus 11.8 ± 2.6 μg/mL, $P = 0.073$; respectively) (Figs. 2C and 2D) were not significantly different.

DISCUSSION

The present study demonstrated that the ARB, valsartan, reduced pro-inflammatory cytokines, TNF-α, and serum IL-6, as well as blood pressure in patients with essential hypertension. It is now well established that inflammation plays a central role in the development of atherosclerosis and its complications. A number of studies have shown that increased blood pressure has an important influence on elevated levels of circulating TNF-α,[2] IL-6,[2,3] and CRP.[4] These pro-inflammatory cytokines and markers induce arterial wall inflammation. Inflammation of the arterial wall causes further damage to the endothelium and elevation of blood pressure, leading to a vicious cycle that promotes atherosclerosis. It may be necessary to reduce inflammation to break this vicious cycle. Moreover, pro-inflammatory cytokines and markers should serve as strong independent predictors of the risk of future cardiovascular events.[19] One of the strategies for the management of atherosclerosis in hypertensive patients is to reduce blood pressure. However, it may be difficult to reduce the serum inflammatory cytokines and markers only by reducing blood pressure. Yasunari et al[20] compared the monocytic reactive oxygen species (ROS) formation and serum CRP between valsartan and amlodipine in hypertensive patients with left ventricular hypertrophy. They showed that the formation of ROS by monocytes was reduced to a greater extent with valsartan than with amlodipine, and that valsartan but not amlodipine reduced CRP levels. Their results indicated that valsartan has an anti-inflammatory action beyond its blood pressure-lowering effect. Fiser et al[18] also reported the anti-inflammatory effect of ARB treatment in patients with essential hypertension. They treated hypertensive patients with the ARB, olmesartan medoxomil, for 6 weeks and

TABLE 1. Characteristics of Subjects

Number (male/female)	29 (16/13)
Age (years)	59.0 ± 14.0
BMI (kg/m^2)	24.2 ± 2.8
Systolic blood pressure (mm Hg)	160.0 ± 16.0
Diastolic blood pressure (mm Hg)	92.0 ± 11.0
Pulse pressure (mm Hg)	67.0 ± 15.0
Pulse rate (/minutes)	71.0 ± 12.0
Total cholesterol (mg/dL)	209.0 ± 28.0
Triglyceride (mg/dL)	184.0 ± 125.0
HDL-cholesterol (mg/dL)	55.0 ± 16.0
HbA1c (%)	5.5 ± 0.9

HDL, high density lipoprotein; HbA1c, hemoglobin A1c.
Mean ± SD.

TABLE 2. Changes in Blood Pressure and Pro-Inflammatory Cytokines and Markers

	Pretreatment	After 3 Months	*P* Value
Systolic blood pressure (mm Hg)	160 ± 16	147 ± 21	0.001
Diastolic blood pressure (mm Hg)	92 ± 11	84 ± 11	0.001
Pulse pressure (mm Hg)	67 ± 15	62 ± 18	0.030
Serum TNF-α (pg/mL)	9.1 ± 8.6	6.1 ± 1.0	0.006
Serum IL-6 (pg/mL)	9.3 ± 1.7	8.9 ± 1.4	0.005
Serum CRP (mg/dL)	1.5 ± 1.0	1.3 ± 0.7	0.424
Serum amyloid A (μg/mL)	13.2 ± 5.6	11.8 ± 2.6	0.073

TNF-α, tumor necrosis factor-α; IL-6, interleukin-6; CRP, C-reactive protein.
Values are expressed mean ± SD.

showed a reduction of serum TNF-α, IL-6, CRP, and monocyte chemotactic protein-1 levels. In the current study, both CRP and SAA tended to be reduced by treatment with valsartan, but the differences did not reach statistical significance. Serum CRP and SAA are acute phase hepatic proteins, stimulated by pro-inflammatory cytokines such as TNF-α, IL-6, and IL-1β. The release of CRP and SAA from the liver may be influenced by various factors, not only vascular inflammation. Previous studies with the ARBs, losartan or candesartan, in patients with coronary artery disease reported no effects of treatment on CRP levels.[21,22] The reason for the discordant effects of treatment with ARBs on CRP levels in different studies is not clear. It is possible that variations in study design or differences among ARBs may have played a role. The mechanisms of the suppressive effect of ARBs on pro-inflammatory action have been discussed. Angiotensin II itself is known to be a pro-inflammatory mediator that causes the release of ROS, including H_2O_2.[23] Therefore, the main anti-inflammatory mechanism of ARBs is inhibition of ROS generation. Indeed, Dandona et al[24] reported that valsartan reduced ROS generation and NF-κB binding activity in mononuclear cells in vivo. It also appears that the use of ARBs increases angiotensin type 2 receptor (AT_2 receptor) activity. Activation of AT_2 receptor increases nitric oxide levels, which may result in diminished cell proliferation and activation of antioxidant properties.[25] Valsartan has a more specific antagonistic action on the angiotensin II type 1 receptor than other ARBs.[26,27] This seems to be a very favorable property of valsartan.

Some studies, including the current study, reported that ARBs decrease TNF-α and IL-6 levels.[18,28] These cytokines are produced mainly in the liver, vasculature, monocytes, and adipose tissues. Recently, Furuhashi et al[29] reported that the ACE inhibitor, temocapril, and the ARB, candesartan, increased adiponectin concentration in patients with essential hypertension. They suggested that the mechanism of this effect was an increase in small insulin-sensitive adipocytes that produce adiponectin. In small insulin-sensitive adipocytes, TNF-α and IL-6 production are diminished more than in large fatty adipocytes, and adiponectin reduces TNF-α and IL-6 production in skeletal muscle cells.[30] Recent clinical trials have suggested that ARBs may reduce the incidence of new-onset diabetes in patients with hypertension.[15] TNF-α impairs insulin action and induces insulin resistance.[31] The decreased production of TNF-α by ARBs may be considered as one of

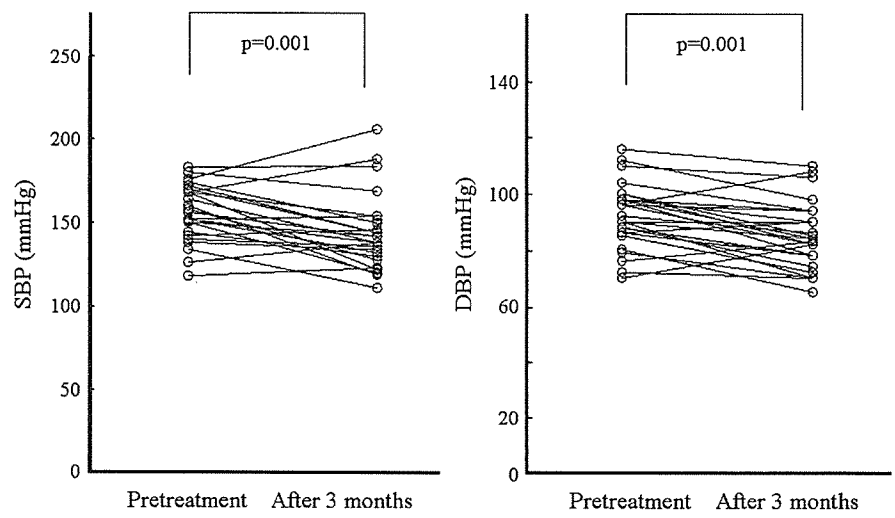

FIGURE 1. Effects of valsartan on systolic and diastolic blood pressure. Three months of treatment with valsartan significantly reduced blood pressure.